GEORGIA INSTITUTE OF TECHNOLOGY
OFFICE OF CONTRACT ADMINISTRATION
SPONSORED PROJECT INITIATION

Date: May 15, 1979

Project Title: Proposal for Modification of ORNL Subcontract No. 3986, Involving Analytic Reactor Physics and Design Investigations

Project No: E-26-645 Steam Cand

Project Director: Dr. J. M. Kallfelz

Sponsor: Union Carbide Corporation, Nuclear Division, Oak Ridge, TN 37830

Agreement Period: From 4/1/79 Until 9/30/79

Type Agreement: Subcontract No. 3986, Supplemental Agreement No. 10 (under DOE Prime No. W-7405-eng-26)

Amount: $68,144

Reports Required: Final Technical Report

Sponsor Contact Person (s):

Technical Matters

C. R. Weisbin
Engineering Physics Division
Oak Ridge National Laboratory
Building 6025, X-10
Oak Ridge, TN 37830

Telecopier No. 615/574-6069
Verification No. 615/574-6068

Contractual Matters
(thru OCA)

Mr. W. R. Osborn
Contract Administrator
Purchasing Division
Union Carbide Corporation
Nuclear Division
P. O. Box M
Oak Ridge, TN 37830

615/483-8611, ext. 34705

NOTE: CONTINUATION OF E-26-610 and E-26-633

Defense Priority Rating: N/A

Assigned to: Nuclear Engineering (School/Laboratory)

COPIES TO:

- Project Director
- Division Chief (EES)
- School/Laboratory Director
- Dean/Director–EES
- Accounting Office
- Procurement Office
- Security Coordinator (OCA)
- Reports Coordinator (OCA)
- Library, Technical Reports Section
- EES Information Office
- EES Reports & Procedures
- Project File (OCA)
- Project Code (GTRI)
- Other

CA–3 (3/76)

GEORGIA INSTITUTE OF TECHNOLOGY
OFFICE OF CONTRACT ADMINISTRATION

SPONSORED PROJECT TERMINATION

Date: December 21, 1979

Project Title: Proposal for Modification of ORNL Subcontract No. 3986, Involving Analytic Reactor Physics and Design Investigations

Project No: E-26-645

Project Director: Dr. J. M. Kallfelz

Sponsor: Union Carbide Corporation, Nuclear Division, Oak Ridge, TN 37830

Effective Termination Date: 9/30/79

Clearance of Accounting Charges: ---

Grant/Contract Closeout Actions Remaining: None

_ Final Invoice and Closing Documents
_ Final Fiscal Report
_ Final Report of Inventions
_ Govt. Property Inventory & Related Certificate
_ Classified Material Certificate
_ Other _____

NOTE: Continued by E-26-601

Nancy

Assigned to: Nuclear Engineering (School/Laboratory)

COPIES TO:

Project Director
Division Chief (EES)
School/Laboratory Director
Dean/Director–EES
Accounting Office
Procurement Office
Security Coordinator (OCA)
/Reports Coordinator (OCA)
Library, Technical Reports Section
EES Information Office
Project File (OCA)
Project Code (GTRI)
Other Research Property Coordinator

CA–4 (1/79)

SCHOOL OF NUCLEAR ENGINEERING

645
E-26-[illegible]

Atlanta, Georgia 30332 (404) 894-3720

17 May 1979

MEMORANDUM

TO: C. R. Weisbin, J. H. Marable* and M. L. Williams (ORNL)

FROM: J. M. Kallfelz, D. Rinaldis, and R. W. Carlson

SUBJECT: Progress Report for ORNL Subcontract 3986
Period April 1-30, 1979

1. Introduction

This belated report is to confirm information already transmitted by phone to Jim Marable and Mark Williams, and to document in detail some of the techniques of LWR modelling we have used. These details, while not appropriate for a report to EPRI, are of interest for our further investigations.

Progress Made: Cell calculations were performed for the Turkey Point PWR to determine 2-group cross sections, and the first rough reactor calculations were accomplished with CITATION. Much has been learned about the problems and techniques of modelling a LWR for such calculations.

Problems

- The appropriate division of the work effort for the joint research with GE has become unclear, because of the uncertainty as to whether GE will receive their requested funding. The associated uncertainty in the level of participation by GE impacts on the role that Georgia Tech should fill, and we propose to redefine this role if GE funding is not assured within one week.

---

* w/o appendices

- o Documentation for the power reactors for which isotopics are to be calculated in the EPRI project has not yet been received. While we presently have plenty to do with the critical lattices, the desired documentation should be obtained shortly for planning. Possibly EPRI CCM-3 is sufficient.

2. Joint Work With GE

No appreciable progress was made on this task in April, for several reasons. During April Dario Rinaldis did not start work on the task until the latter half of the month, and his time was spent on familiarizing himself in detail with some of the theoretical aspects of this work. Further, because of the uncertainty about the level of GE participation mentioned in section 1, we felt it unwise to invest much time in this project until our priorities are clear. E.g., if G. E. does receive funding they would handle the major COROPT runs. This influences the priority of initiating at ORNL the new version, COROPT-I [1].

3. PWR Calculations

Using the documentation for the Turkey Point #3 Reactor [2] supplied by Odelli Ozer, we have performed some preliminary calculations for the first cycle of this reactor. This reactor is a relatively small (2200 MWth, ~ 750 MWe) Westinghouse reactor located at Miami.

We have established that we can perform runs on the Berkeley CDC, by performing a TRX-2 run supplied by Vann Baker. We then attempted an EPRI-CELL calculation using the sample input given in [2], but the execution was only partically completed due to an error. Lacking the necessary information for the Berkeley version to locate the error, we decided to delay further EPRI-CELL runs until the ORNL version was operational.

Meanwhile, we generated 2 group cross sections by performing cell calculations for the various fuel pins and burnable poison rods, using MACH 1 [3] and the 26 group Bondarenko cross section set (ABN) [4] for the fast range (1 eV - 10.5 MeV) and THERMOS [5] for the thermal range. Details for mock-up of one of these cells is included in Appendix I.

For the MACH calculations we also obtained a "thermal" group value, which included groups 23-26 of the ABN set. Group 26 is the 2200 m/s value, and contains no spectral correction. Thus, as expected, the THERMOS σ_a values for the thermal group were generally about 20% lower than the MACH results. Exceptions were isotopes such as Pu-239; because of its large resonance at about 0.3 eV, its THERMOS σ_a value was higher than the MACH value, because of the hardened spectrum. Figure 1 gives the spatial dependence of ϕ for several thermal energies, for the 3.1% enriched outer core fuel pin.

The entire reactor was then modeled in R-Z geometry, and the first 417 day cycle was calculated with CITATION [6]. Some details of this model are given in Appendix II.

The model has some rough approximations, and is still being improved and debugged, in on-going calculations. However, considering the approximations made, the results are encouraging. k_{eff} at BOL is about 0.95. The Δk during the cycle is about 9%, agreeing well with the experimental value, and the EOC Pu-239/U-235 power ratio is about 50/50, typical of a PWR.

4. Thermal Transport Cross-Sections in EPRI-CELL

I have not yet had time to study the problems discussed by R. E. MacFarlane [11] in detail, but plan to do so. Nonetheless, following are some rather spontaneous comments which I believe are pertient to the problem.

(a) Frankly, I am suprised that the transport corrections were applied to the σ_t used in the THERMOS solution. It seems clear that this will influence the THERMOS solution convergence, etc. As pointed out by MacFarlane, the original THERMOS program [7] solves equations which were developed for isotropic scattering, and I can find nothing in the EPRI-CELL documentation which indicates any changes in this basic assumption. The general development of the THERMOS equations is outlined in Appendix III. Thus, if σ_{tr} is placed in the σ_t position used in the THERMOS solution, it seems likely that inconsistencies will be encountered. It is my opinion that σ_{tr} should be used in THERMOS only in the group cross section edit, and I have more comments on this in (c) below.

Thus I agree with what I believe is one of MacFarlane's conclusions in his March 30 letter, that only P_o cross sections should be used in the THERMOS solution. Furthermore, it does not seem suprising that, as mentioned in his April 18 letter, "The THERMOS calculation still refuses to converge with transport corrected data."

(b) Possibly there is some approximation which allows a transport cross section to appear in the THERMOS formalism, e.g. by diagonalizing the $\Sigma_1(E' \rightarrow E)$ matrix [9], but if so I have not yet found it.

(c) As MacFarlane points out, data from EPRI-CELL is to be used in diffusion codes. As discussed succintly by Travelli [12], using only $\phi(E,\vec{r})$ there is no truly correct way to collapse the microscopic transport cross sections, so that they are consistent with the definition of the macroscopic value, Σ_{tr}. This is related to the fact that $D(E) \sim 1/\Sigma_{tr}(E)$ in what appears in the diffusion equation. Several popular options for σ_{tr} averaging are [3,11]

$$\langle \sigma_{tr} \rangle_g = \frac{\phi_g}{\int_g \frac{\phi(E)}{\sigma_{tr}(E)}\, dE} \qquad (1)$$

and

$$\langle \sigma_{tr} \rangle_g = \int_g \sigma_{tr}(E)\ \phi\ (E)dE \qquad (2)$$

where g and $\int_g$ refer to group g and the integral over its energy range.

Definition (1) is generally considered more appropriate for diffusion theory calculations, because it at least gives more importance to the energy range where $\sigma_{tr}(E)$ is small, as should D_g. Equation (2) is more appropriate for transport theory, but it is the expression used to determine the THERMOS "output" which is used in diffusion theory.

(d) Based on comments (a) and (b), trying to make a transport correction in THERMOS seems inconsistent, and results with such corrections are suspect. Thus a comparison between results with and without such a correction are presumably not appropriate to draw conclusions about the importance of the inclusion of P_1 scattering, if it were possible.

The small pin fuel-water "interface" problem is of course not equivalent in detail to the Milne problem for a quasi-infinite H_2O slab, but it does have many similarities.

For calculations I did at Karlsruhe eons ago [9], the average energy of the thermal spectrum leaking from the H_2O into the vacuum was 3-4% lower for the isotropic scattering assumption than for calculations including the full $\Sigma_1(E' \rightarrow E)$ matrix. The latter calculations agreed well with experiments [10].

However, generally the gradients in the cell problem are not as strong as for the Milne problem. Honeck supports the accuracy of the isotropic scattering approximation as follows:

> "We define the birth-rate (or emission) density as [equation given] which is the angular distribution of neutrons following a collision. The birth rate density will be nearly isotropic if either the scattering process is nearly isotropic or the neutron density is nearly isotropic. Both of these conditions are reasonably well satisfied since the scattering kernel for thermal neutrons is more isotropic than for high energy neutrons due to thermal motion and binding, and the gradients (and hence the anisotropy) of the flux in a lattice is generally small." [7].

FIG. 1. THERMOS RESULTS FOR 3.1 w/o ENRICHED FUEL PIN CELL. (V values in units of 2200 m/s) Operating temperature.

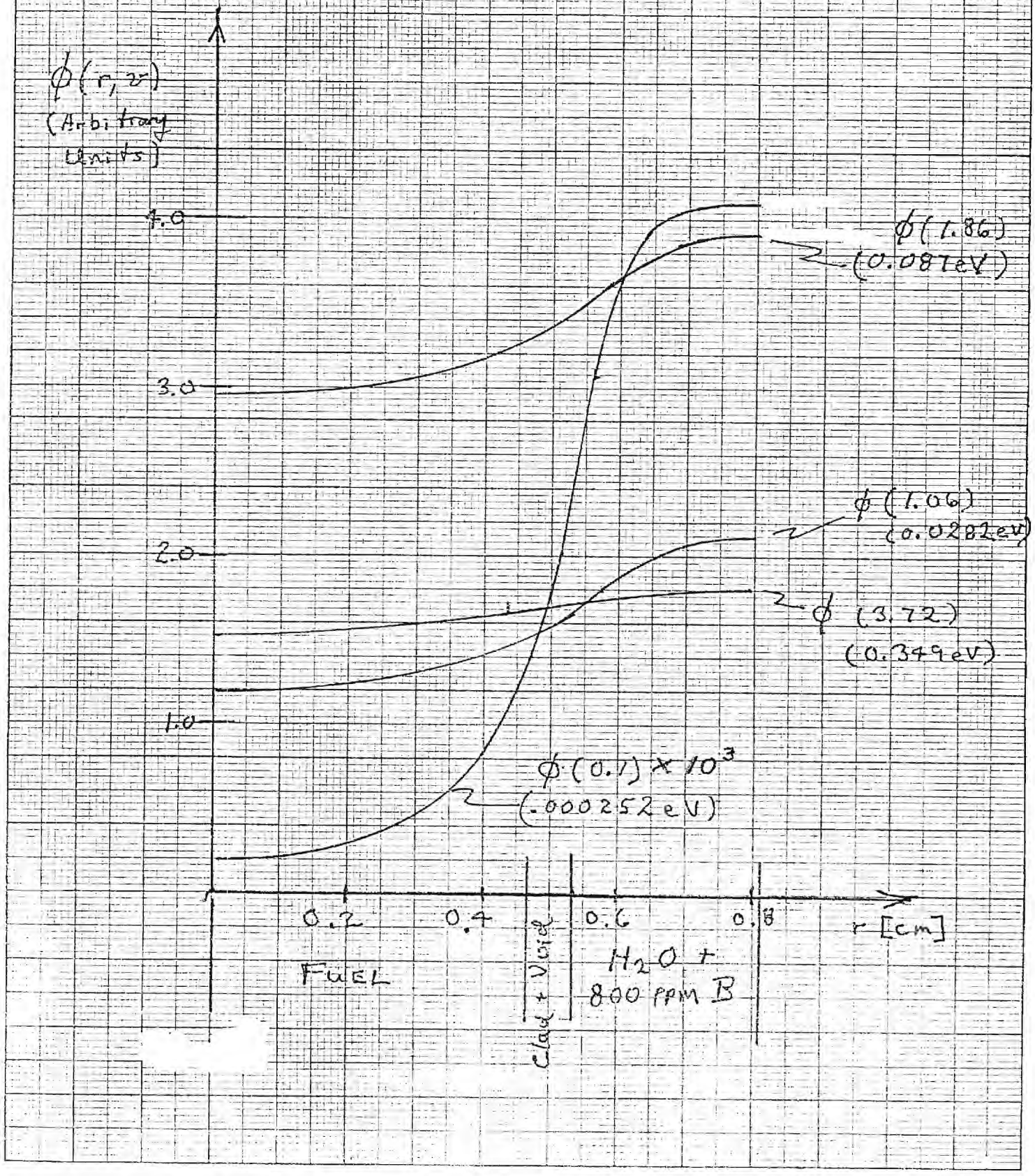

References

[1] Private communication from Mary Caramena-Hittle (GE-ARSD) to J. M. Kallfelz, February 28, 1979.

[2] "Reactor Core Physics Design and Operating Data for Cycles 1, 2, and 3 of the Turkey Point #3 PWR Power Plant," NP-827, Electric Power Research Institute, July 1978.

[3] D. A. Meneley, et al., "MACH 1, A One-Dimensional Diffusion Theory Package," ANL-7223, June 1966.

[4] L. P. Abagyan, et al., Group Constants for Nuclear Reactor Calculations, Consultants Bureau, New York, 1964.

[5] B. J. Toppel and I. Bakys, "The Argonne-Revised Thermos Code," ANL-7023, 1965.

[6] T. B. Fowler, et al., "Nuclear Reactor Analysis Code: CITATION," ORNL-TM-2496, Rev. 2, July 1971.

[7] H. C. Honeck, "Thermos, A Thermalization Transport Theory Code for Reactor Lattice Calculations," BNL-5826, September 1961.

[8] R. Kladnik and I. Kuščer, "Milne's Problem for Thermal Neutrons in a Nonabsorbing Medium," Nucl. Sci. Engr. 11, 116, October 1961.

[9] J. M. Kallfelz and W. Reichardt, "An Improved Variational Solution to the Energy-Dependent Milne Problem for Realistic Scattering Kernels," Nukleonik 9, 148, 1967.

[10] J. M. Kallfelz, "Experimental Investigations of Angular Dependent Thermal Neutron Leakage Spectra," Nukleonik 9, 277, 1967.

[11] R. E. MacFarlane, LASL, letters to O. Ozer, EPRI, dated March 30, 1979 and April 18, 1979.

[12] A. Travelli, "A New Formulation of Multigroup Microscopic Cross Sections," in "Reactor Physics Div. Annual Report, July 1, 1967 to June 30, 1968," ANL-7410, p. 413 (January 1969).

Progress Report to ORNL
17 May 79

APPENDIX I. Modeling Turkey Point 3 Cell for THERMOS Input

Cell Modelled: 3.1 w/o Enriched fuel pin, used in core outer region. See item 5, Table 2.2 of [2].

(a) Fuel Rod

O.D. = 0.3649" $\Rightarrow$ $r = 0.4634$

Assuming dishing fraction = 0.02

$$N_{UO_2} = \frac{\rho a}{A} = \frac{(10.08)(.98)(.6023)}{270} = 2.2036 \cdot 10^{-2}$$ molecules/bn-cm

$N_u = N_{UO_2}$ $\quad N_o = 2 \cdot N_{UO_2}$

Enrichment to atom fraction conversion:

$$3.10 = \frac{235\,x}{235\,x + (1-x)238} \cdot 100 \text{ , where } x = \frac{N^{25}}{N^{25} + N^{28}}$$

$x = 3.1383 \cdot 10^{-2}$

$\Rightarrow$ $N^{25} = 6.9156 \cdot 10^{-4}$ atoms/bn-cm
$N^{28} = 2.1344 \cdot 10^{-2}$ "

Note: Assumption which works pragmatically is that there are no temperature-induced dimension changes in solid components of core.

(b) Clad

(Homogenize clad & gap because neither are important)

Clad O.D. = .422 in ⇒ clad + gap thickness = .0725 cm.
clad " = .0617 cm

$$N_{Zr} = \frac{\rho Q}{A} = \frac{(6.56)(.6023)}{91.22} = 4.3314 \cdot 10^{-2} \text{ atoms/bn cm, in clad}$$

Homogenized $N_{Zr} = (4.3314 \cdot 10^{-2})\frac{.0617}{.0725} = 3.6875 \cdot 10^{-2}$

Note: This assumes the clad to be all Zr, and trace allowing elements are ignored. To include " " " one can adjust the Zr concentration to give the correct Σ_a.

(c) Moderator with Boron

Convert square into equivalent circular region; with diameter d_e
Fuel pin pitch = 0.563 in. See item 4, table 2.2 of [2].

$$.563^2 = \frac{\pi}{4} d_e^2 \Rightarrow d_e = .6353 \text{ in}$$

$$\text{Thickness} = (.6353 - .422)\frac{2.54}{2} = .2709 \text{ cm}$$

Concentrations

For cold conditions, $\rho = 1.0$ g/cc

$N_H = (6.692 \cdot 10^{-2})(.9962)$ $N_0 = (3.346 \cdot 10^{-2})(.9962)$
where .9962 is reduction for spacer, to be discussed below

For hot conditions, $\bar{T} = 575.4°F$ $p = 2250$ psia
$\rho_{H_2O} = 0.7079$ g/cc

continuing ⓒ Moderator

∴ For hot conditions $N_H = 4.719 \cdot 10^{-2}$ atoms/bn-cm
$N_O = 2.360 \cdot 10^{-2}$ "

Boron

At BOL, H_2O has 800 ppm natural boron

$$800 \cdot 10^{-6} = \frac{(N_B)((10.811)}{(N_B)(10.811) + (N_{H_2O})(18)}$$

$$\Rightarrow \frac{N_B}{N_H} = 1.333 \cdot 10^{-3}$$

$$\therefore N_B = 4.443 \cdot 10^{-5}$$

ⓓ "Extra Regim"

This regim can be used to include materials (i.e. fuel assembly materials, H_2O between assemblies) not clearly associated with a pin.

For our runs this was not considered, except that of course the smeared number densities for the reactor regions were different than those for the THERMOS cell.

ⓔ Heavy Scattering Ring

This is used in THERMOS as an artificial region to correct the boundary condition to one of isotropic return rather than mirror image return. I.e., this avoids the possibility of neutrons with low incidence angle to the boundary just continuously bouncing off the boundary, by adding a ring of heavy (∴ isotropic) scatterer.

This option is included in EPRI-CELL, which has also been improved to include an analytic isotropic boundary condition. See p. 5-26 of the EPRI-CELL documentation for a discussion of the two alternate methods for the boundary condition.

LASER recommends that the neutronic thickness of this ring be two mean free paths, and that the mesh spacing be that of the previous region. (.0226 cm for our case). Using a $\sigma_s = 10$ bn:

$$\Sigma = 1/.0226 = N\sigma = 10 \cdot N,$$

from which N can be determined.

(f) Inclusion of Spacer

See diagram 2.2-9 of [2] for location of spacer.

Each spacer weighs about 13 ounces., and is made of Inconel 718, with $\rho = 0.296$ lb/in^3.

$\therefore$ Volume is $(13/16)/.296 = 2.745$ in$^3 = 44.98$ cm^3

This volume is to be roughly proportional over the water volume in an assembly in a section whose length is the average spacer separation. This varies from ~ 19 - 26", according to the diagram referenced above. We mistakenly assumed 18" for this value but the correction is minor, and the method is as follows.

With 225 rods/asby, the

$$\text{Vol } H_2O = [\underbrace{.563^2}_{\text{see (c)}} - \underbrace{.422^2 \tfrac{\pi}{4}}_{\text{see (b)}}](225)(18) = 717.3 \text{ in}^3$$

(f) Spacer (continued)

∴ Vol. fract. H_2O = .9962
" " Spacer = .00383

To mock up Inconel, we used the following Tedious process, which can be avoided by using the "Engineering Input" of EPRI-CELL. As can be seen, many trace elements could be ignored.

Inconel 718 Composition

	w/o	σ_a (2200 m/s)
Ni	52.5	4.6
C	0.04	~0
Mn	0.20	13.44
Fe	18.5	7.55
S	0.007	~0
Si	0.30	~0
Cu	0.07	3.79
Cr	18.6	3.10
Al	0.40	0.23
Ti	0.90	6.10
Nb	5.0	1.06
Mo	3.1	2.70

Using this information, plus atom concentration of pure Inconel 718 = 0.08299 atoms/bn-cm

σ_a (2200) = 3.685 barns for "average" In 718 atom

For THERMOS, smeared $N_{In\,718} = 3.179 \cdot 10^{-4}$ atoms/bn cm

Note that often many isotopes can be conveniently lumped together in THERMOS, assuming they all have $\sigma_a \sim 1/v$.

APPENDIX II. Modeling the Turkey Point 3 Reactor for CITATION Calculations

This appendix will not cover modeling minutiae, as in the previous appendix. It will give some general comments about modeling the reactor, as well as some details about the upper and lower axial reflectors, which may be of interest for future calculations. Apparently our near-term effort will concentrate on pin and assembly calculations with EPRI-CELL and EPRI-CPM, based on our revised program plan.

① Geometry Used

For the first calculations we selected an R-Z geometry, to allow a "3-D" calculation with a "2-D" run. In retrospect, given the checkboard arrangement of two different type assemblies in the inner core zone, perhaps an X-Y calculation with a B_z^z would have been preferable. Diagram 2.2-1 of [2] shows the BOL

arrangement for the first cycle. The two main types of assemblies in the inner core are those with 1.86 w/o rod enrichment, and those with 2.56 w/o " " plus 12 burnable poison rods per assembly.

For the inner core we maintained the volume of these assemblies in R-Z geometry, and calculated the volume-averaged number densities, based on the various constituent assemblies.

The "outer core" ring had the same volume as all of the 3.1 w/o assemblies shown in the diagram 2.2-1 of [2].

Based on the many approximations we made, the results for this model were reasonably good, as mentioned in the body of the report.

(5) Number Densities

While this may seem trivial, the usual problems were encountered. Several points to keep in mind are as follows:

(i) THERMOS prints macroscopic average Σ values. To obtain the microscopic σ values for CITATION, one should divide the cell-averaged Σ by the volume-averaged N_i for the THERMOS cell. The region-averaged Σ from THERMOS are of interest, but are not appropriate for CITATION input.

(ii) The CITATION number densities should of course be determined including all the materials of the region. Only if one assumes a CITATION region to consist only of one particular type THERMOS cell, and the THERMOS cell contains the "extra region" mentioned in ② of Appendix 1, will the CITATION N_i's be the same as those for THERMOS mentioned in (i). If these conditions are fulfilled, one could in principle use $N = 1$ for THERMOS and CITATION, although the burn-up results would of course have to be interpreted with care.

③ Reflectors

The dimensions of the radial reflector are well-defined by the core barrel (see Diagram 2.2-5 of [2]).

However, the axial reflectors are not well-defined, since there is H_2O and structure for a large distance above and below the active core. Thus the questions of interest are

(i) How large should the axial reflector be so that a further increase in thickness would not influence the calculations for the core appreciably?

(ii) What should the composition of the reflectors be?

Question (i) can be studied by considering the Fermi age, τ, and the

migration area, $M^2 = \tau + L_{th}^2$.

However, pragmatic usage is that 8-10 in and ~7 in are appropriate for the lower and upper reflectors, respectively.

Compositions

Lower reflector A typical approximation is that this reflector is 50% H_2O and 50% stainless steel. this is an approximation to various components:

Diagram 2.2-9 of [2] shows the lower part of an element. Below the active fuel in the pin there is about 3/4" consisting of an insulator (Al_2O_3) and Zirc plug. Below that is the bottom nozzle, about 2.7" long, which rests on the lower core plate. Diagram 2.2-6a shows the lower core plate (several inches thick and perforated with many H_2O-filled holes) as well as the rest of the lower core support assembly.

Upper Reflector

Typically the composition of this reflector is assumed to be that of a fuel element, without the fuel. As mentioned in Table 2.2 of [2], there is a 7" "unheated length" at the top of the fuel pin. This consists of an insulator, an essentially void region which has only a stainless steel spring, and a Zirc plug. Also, at BOL there is about one inch between the tops of the pin and the top of the assembly, to allow for pin "growth".

APPENDIX III. Integral Transport Theory With Isotropic Scattering

Consider simplified case, one of those treated by THERMOS [7]:

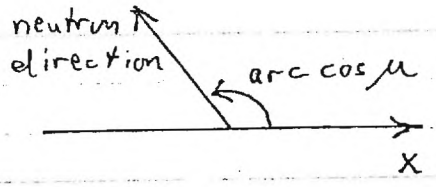

(a) "Infinite slab"

(b) No fission or fixed source

(c) Ignore "high E" source (considered in THERMOS, but doesn't change argument.

For this case the transport eqn has the following form [8, 9]

$$\left[\mu\frac{\partial}{\partial x} + \Sigma_t(x';v)\right]\phi(x';v,\mu) \qquad (1)$$

$$= \underbrace{\int_0^\infty \int_{-1}^{1} \Sigma(x';v';\mu' \to v,\mu)\,\phi(x';v';\mu')\,dv'd\mu'}_{F(x';v,\mu)}$$

An integrating factor for the l.h.s. of (1) is used to develop integral transport theory:

$$\text{I.F.} = e^{\frac{x'\Sigma_t}{\mu}} \qquad (2)$$

Multiply (1) by I.F., integrate $\int_{\eta(\mu)}^{x}$

where $\eta(\mu) = \begin{cases} -\infty, & \mu > 0 \\ \infty, & \mu < 0 \end{cases}$ (3)

Result:

$$\phi(x,v,\mu) = \int_{\eta(\mu)}^{x} F_1(x';v,\mu)\, e^{-\frac{\Sigma_t(x-x')}{\mu}} \frac{dx'}{\mu} \quad (4)$$

Use Legendre expansion: [8, 9]

$$\Sigma(v',\mu' \to v,\mu) = \tfrac{1}{2} \sum_{n=0}^{N} (2n+1)\, \Sigma_n(v' \to v)\, P_n(\mu)\, P_n(\mu') \quad (5)$$

where it can be shown that the Σ_n are the same as those in the expansion for the angle between the initial and final direction, μ_0: [8]

$$\Sigma(v' \to v;\mu_0) = \frac{1}{4\pi} \sum_{n=0}^{N} (2n+1)\, \Sigma_n(v' \to v)\, P_n(\mu_0) \quad (6)$$

To get equation solved by THERMUS assume isotropic scatter:

i.e. Σ_n in eqns (6) and (5) $= 0$ for $n \neq 0$

then $F_1(x';v,\mu) = \int_0^{\infty}\int_{-1}^{1} \tfrac{1}{2}\Sigma_0(v' \to v)\, \phi(x',v',\mu')\, dv'd\mu'$

or $F_1 = F_1(x',v) = \frac{1}{4\pi}\int_0^{\infty} \Phi(x',v')\, \Sigma_0(v' \to v)\, dv' \quad (7)$

The significant point is that by assuming isotropic scatter, the r.h.s. of (4) now involves the "total" flux, $\Phi(x',v')$ rather than

the angle-dependent $\phi(x;v',\mu')$. Thus, to obtain an expression for $\underline{\Phi}(x,v) = 2\pi \int_{-1}^{1} \phi(x,v,\mu)\,d\mu$, Eqn (4) is integrated to obtain:

$$\underline{\Phi}(x,v) = \frac{1}{2}\int_{-1}^{1} d\mu \int_{\eta(\mu)}^{x} \left\{ \left[\int_0^\infty \underline{\Phi}(x';v')\,\Sigma_0(v'\to v)\,dv' \right] \cdot \exp\left[-\frac{\Sigma_t(x-x')}{\mu} \right] \right\} \frac{dx'}{\mu} \qquad (7)$$

This is the basic form of the eqn. solved by THERMOS. (I wouldn't bet on the constants, since this was done hurriedly, and they're not significant to the argument.)

The significant point is that by introducing the isotropic scatter, the THERMOS integral transport eqn. contains only the scalar $\underline{\Phi}(x,v)$ – see eqn. (7). $\phi(x,v,\mu)$ is not calculated or used.

SCHOOL OF NUCLEAR ENGINEERING

Atlanta, Georgia 30332 (404) 894-3720

E-26-645

June 6, 1979

MEMORANDUM

TO: C. R. Weisbin, J. H. Marable and M. L. Williams (ORNL)

FROM: J. M. Kallfelz and D. Rinaldis

SUBJECT: Progress Report on Work for ORNL
Subcontract 3986, Period May 1-31, 1979

1. Summary

The work described in this memorandum is related both to investigations of LMFBR performance with COROPT, and calculations of the Turkey Point 3 PWR. Accomplishments this month have been:

o A model of the PRPCDS reactor has been developed for use in Sensitivity Analysis related to COROPT.

o Areas which could lead to inconsistencies between the COROPT reactor model and that used in the sensitivity codes have been identified.

o A comparison has been made between the COROPT results and those from a GE neutronics code, for the PRPCDS reference reactor.

o We have improved the model and cross sections used to calculate the Turkey Point 3 PWR first cycle with CITATION, and some comparisons between calculations and experiments are reported.

Plans for next month's work:

o We have proposed a series of relatively simple calculations, using many results already at hand, to illustrate the influence of correlation between integral parameters on the estimated variance of costs.

o Work utilizing EPRI/CELL to analyze BAPL-1 has just been initiated, and will be continued. Particular attention will be paid to problems of convergency in the ORNL code version, and to the consistency of results for the general and engineering input cases, as well as their consistency with results for other codes such as THERMOS.

2. COROPT Input Analysis

Before beginning a detailed description of topics that we have investigated and that have involved COROPT [1] runs it is appropriate to describe the principal characteristics of the COROPT input for the nuclear parameters. In fact the one peculiarity of the method utilized in this code is the impossibility of the designer's direct specification of several parameters which can be input in neutronics codes such as CITATION. Several examples of this characteristic are given below.

2.1 Enrichment

The core zone enrichments are determined with the correlation given on page 4-24 of Reference [1], which involves volume fractions of the various components, geometric information, and data related to the cycle length and power. These enrichments are determined at BOEC and at EOEC.

2.2 Thermal Power

The thermal power, which influences the burn-up characteristics, is also not directly controlled by the input. Rather, it is calculated from the required electrical power, and the pumping power which is determined by various input parameters such as the assembly design, core ΔT, etc.

2.3 Loading Zones

Figure 4.5 of Reference [1] shows the R-Z model used in COROPT for the burn-up calculations. Nine different loading zones can be used, with 3 zones each for the core, radial blanket and axial blanket regions. However, the user can control the geometry and BOL enrichment only of two core zones, while for the other regions the user can only specify the homogeneous region size. The code then subdivides the regions into zones.

2.4 Control Rods

In the R-Z model apparently the contol rods are not explicitly included. However, input includes control rod description, which is used to determine the appropriate region volume fractions for fuel, structure, etc. for the criticality calculation.

3. A Consistent Model for the PRPCDS Reactor

In our May 14 Memorandum [2], we proposed a GE $(PuU)O_2/UO_2$ reference model for the Proliferation Resistant Preconceptual Core Design (PRPCDS) [3-5] for studies of the impact of design data uncertainties on reactor performance. Several points were outlined concerning consistency of the above model with the COROPT model. Further investigations are necessary to insure the consistency of our model for some other parameters.

To examine the consistency of the COROPT model and performance parameters with those for a neutronics code [3], we performed a COROPT calculation for the PRPCDS model and made more complete investigation of the results than was done previously [6]. Because of differences in the cross section data used in [3] and to obtain the correlations in [1],

some differences would be expected. Furthermore, Ed Kujawski [7] has indicated that there are some errors in the results of [3], (the reported breeding ratio is several % high, while the cycle fissile gain is believed to be about 15% too large) so a comparison with these values cannot be conclusive.

Table 1 shows the difference in the enrichment values and a comparison between GE [3] and COROPT results for the most interesting nuclear parameters. While a closer agreement would be desirable, the differences for most parameters are small, especially if we assume that the fissile mass loading for COROPT does not include U-235.* Thus for the parameters we have considered it appears that the results of the old version of COROPT [1] are sufficiently consistent with other results for initial investigations of the topics proposed for joint work with GE.

4. Calculations Proposed to Illustrate the Influence of Correlation between Integral Parameters on the Variance of Costs

A general expression for the variance of the cost due to integral parameter uncertainties is given in Reference [8] as:

$$VAR(\$) = \sum_{i,j} \frac{\partial \$}{\partial I_i} \frac{\partial \$}{\partial I_j} COV(I_i, I_j) \qquad (1)$$

where \$ is a cost, $I_{i,j}$ represent the integral parameters and $COV(I_i, I_j)$ is the convariance matrix that takes in account the correlation between I_i and I_j.

The following expression is also given in [8]:

$$COV(I_k, I_h) = \sum_{i,j}' \frac{\partial I_k}{\partial \sigma_i} \frac{\partial I_h}{\partial \sigma_j} COV(\sigma_i, \sigma_j) \qquad (2)$$

---

* A subsequent examination of the code verified that the COROPT fissile mass indeed includes only plutonium.

Table 1 Comparison between several nuclear performance parameters calculated by COROPT and those reported in Reference [3].

Performance Parameter	GE	COROPT
Thermal Power (MWt)	2740	2754
Breeding Ratio	1.32	1.31
Doubling Time (years)	15.0	15.0
Enrichment core zone 1 BOEC/EOEC* (%)	10.5/10.9	9.9/10.0
Enrichment core zone 2 BOEC/EOEC (%)	14.1/12.4	13.8/12.7
BOEC Fissile Mass** (kg)	3635(3485)	3392
Fissile GAIN/cycle (kg)	308	295

*The results printed in the COROPT output indicate that these are BOL and EOL values, but an examination of the code shows that they are calculated for the BOEC and EOEC.

**The value in brackets, is the value without U-235 contribution.

The objective of our calculations will be to evaluate, by COROPT runs, the sensitivity coefficients $\frac{\partial \$}{\partial I_k}$ and $\frac{\partial \$}{\partial I_h}$ where I_k and I_h are the breeding ratio and the enrichment, while \$ represents one of the costs determined by COROPT, i.e. the fuel cycle cost.

We propose that the calculation of the covariance matrix, Eq. (2), will be the principal Oak Ridge contribution to this work. To obtain useful illustrative results quickly, we suggest that Oak Ridge calculate the covariance matrix, Eq. (2), for the integral parameters utilizing the covariance data files and sensitivity coefficients already calculated for the LCCEWG reactor in Reference [9]. In this study calculations were performed for the sensitivity coefficients of the breeding ratio and k, and we would like this information for the BR both with and without k-reset; we believe the latter is consistent with COROPT.

The results of these calculations will be related to enrichment charges utilizing a simple proportionality factor for the enrichment and k, also to be calculated by ORNL.

Equation (1) can then be used to calculate a cost "variance", employing cost sensitivity coefficients to be calculated at Georgia Tech with COROPT. Naturally this will not be the true variance, since we have not included all the significant parameters.

However, a comparison of the results of Eq. (1) with a simpler equation given in Reference [8] which ignores integral parameter correlations

$$SD(\$) = \left\{ \sum_i \left[\frac{\partial \$}{\partial I_i} SD(I_i) \right]^2 \right\}^{\frac{1}{2}} \qquad (3)$$

should be of interest because the two results will illustrate clearly the impact of integral parameter correlations on economic uncertainty calculations. It should be noted that Eq. (3) is similar to expressions used in earlier studies [10], which did not include correlation effects. Further, the $SD(I_i)$ terms are part of the covariance matrix we request ORNL to calculate.

The goal of this work is to have these calculations completed soon enough so that an ANS summary can be mailed by 22 June, for presentation at the San Francisco ANS meeting.

5. Analysis of the Turkey Point 3 PWR

5.1. Calculational Methods

As discussed in last month's progress report [11], cell and reactor calculations have been performed for the Turkey Point 3 PWR, using documentation provided by EPRI [12]. The model used has been improved and debugged this month.

The codes MACH 1 [13] and THERMOS [14] were used to generate two-group cross section sets for the various regions of this reactor, as described in [11].

The entire reactor was then modeled in R-Z geometry, and the first 417 day cycle was calculated with CITATION [15]. Two core zones were considered:

(a) the "inner core" is composed primarily of two types of fuel assemblies (see diagram 2.2-1 of [12]). Fifty three of these elements have a fuel enrichment of 1.86 w/o, while 52 are "type 2" assemblies with 2.56 w/o fuel enrichment and 12 burnable poison rods per assembly.

This zone was homogenized into a zone with an average fuel enrichment of about 2.2 w/o, with the burnable poison smeared over the region.

(b) the outer core consisted of 52 fuel assemblies, 16 of which also contained burnable poison rods.

The details of the reflector modeling have been described in [11].

For the burnup calculations, the following approximations were made:

(a) To a first approximation, burnable poison burn-up and fission product generation compensate each other. Therefore, in our model fission products were not considered, nor was the burnable poison depleted.

(b) The soluble boron was kept at its BOL concentration (800 ppm) during the entire cycle, rather than searching for its concentration to maintain criticality at each time step.

(c) Normally one bank of control rods is inserted about 10% into the core during operation. However, we could find no definite information on this topic in the documentation, and ignored the control rods in the calculations.

Of course, the two primary fuel chains, i.e. burn-up of U-235 and breeding of plutonium through Pu-242, were considered.

5.2. Comparison with Experiment

5.2.1. k_{eff}

The BOL initial calculated k_{eff}, with burnable poison and soluble poison included, was slightly greater than 1.0; the input enrichment was reduced about 1.5% in the search for criticality at BOL. Considering the approximations made to generate the cross section set, this result is surprisingly good.

The calculated Δk during the cycle was 7.9%. This is to be compared with an experimental value of about 10%, based on the average value of the soluble boron worth from the hot zero power experiments, and a boron concentration decrease of about 750 ppm as obtained from the boron let-down curve for the cycle. Inherent in this comparison is the assumption stated above that the burnable poison depletion and fission product build-up approximately compensate each other.

5.2.2. Power Distributions

Diagram 2.4-2 of [12] provides experimental radial and axial power distributions. Since the inner core consists of a "checkboard" arrangement of several types of assemblies, the power values at different points the same radius from the core center will scatter somewhat. A detailed comparison with the results of our R-Z model is thus not particularly meaningful, since the "average" values at different radii from the core center are difficult to define. Furthermore, our model apparently still needs some refining, since at BOL the inner core power density was too low compared to that in the outer core, and actually sloped slightly toward the core center.

We calculated only 1/2 the core, so our calculated axial profiles are symmetric about the core midplane. Nonetheless, an examination of calculated and experimental axial distributions shows several interesting phenomena. For the curves discussed below, the experimental values are the average of the results from detectors 20 and 28, both located in fuel elements in the corners of the square of eight elements surrounding the core central element. The calculated values are arbitrarily normalized to show the differences in the calculated and experimental shapes clearly,

Figure 1 compares BOL axial power profiles. The "skew" of the curve toward the top half of the core would of course not be calculated, for the reason mentioned above. However, the physical reason for this skew is not understood. I have discussed this behavior at length with several PWR experts, particularly Roger Carlson. Roger was quite surprised at this behavior and said that all the physical phenomena he is familiar with would predict a skew toward the bottom of the reactor!

Figure 2 shows that our calculations failed notably to predict the EOC power depression at the core center. We treated fuel burn-up and breeding properly, so presumably this failure is caused by our assumptions about burnable poison and fission products, mentioned in 5.2.1. While their depletion and build-up, respectively, may approximately compensate for each other on a global basis, this is presumably not true locally. For our ARMP calculations these effects will of course be treated accurately.

Fig. 1. BOL AXIAL POWER DENSITY SHAPE

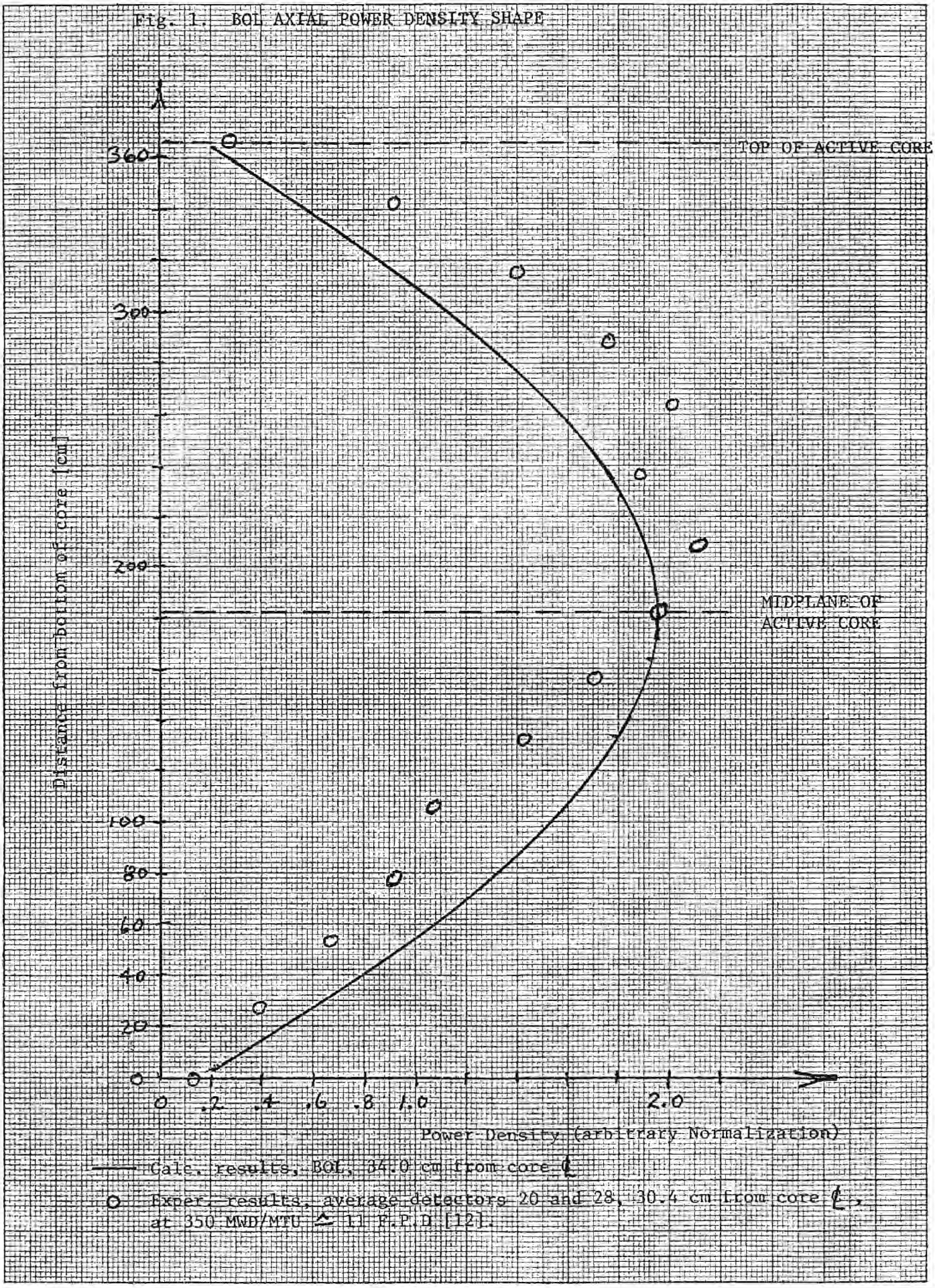

—— Calc. results, BOL, 34.0 cm from core ℄

O Exper. results, average detectors 20 and 28, 30.4 cm from core ℄, at 350 MWD/MTU ≙ 11 F.P.D [12].

Fig. 2. EOL AXIAL POWER DENSITY SHAPE

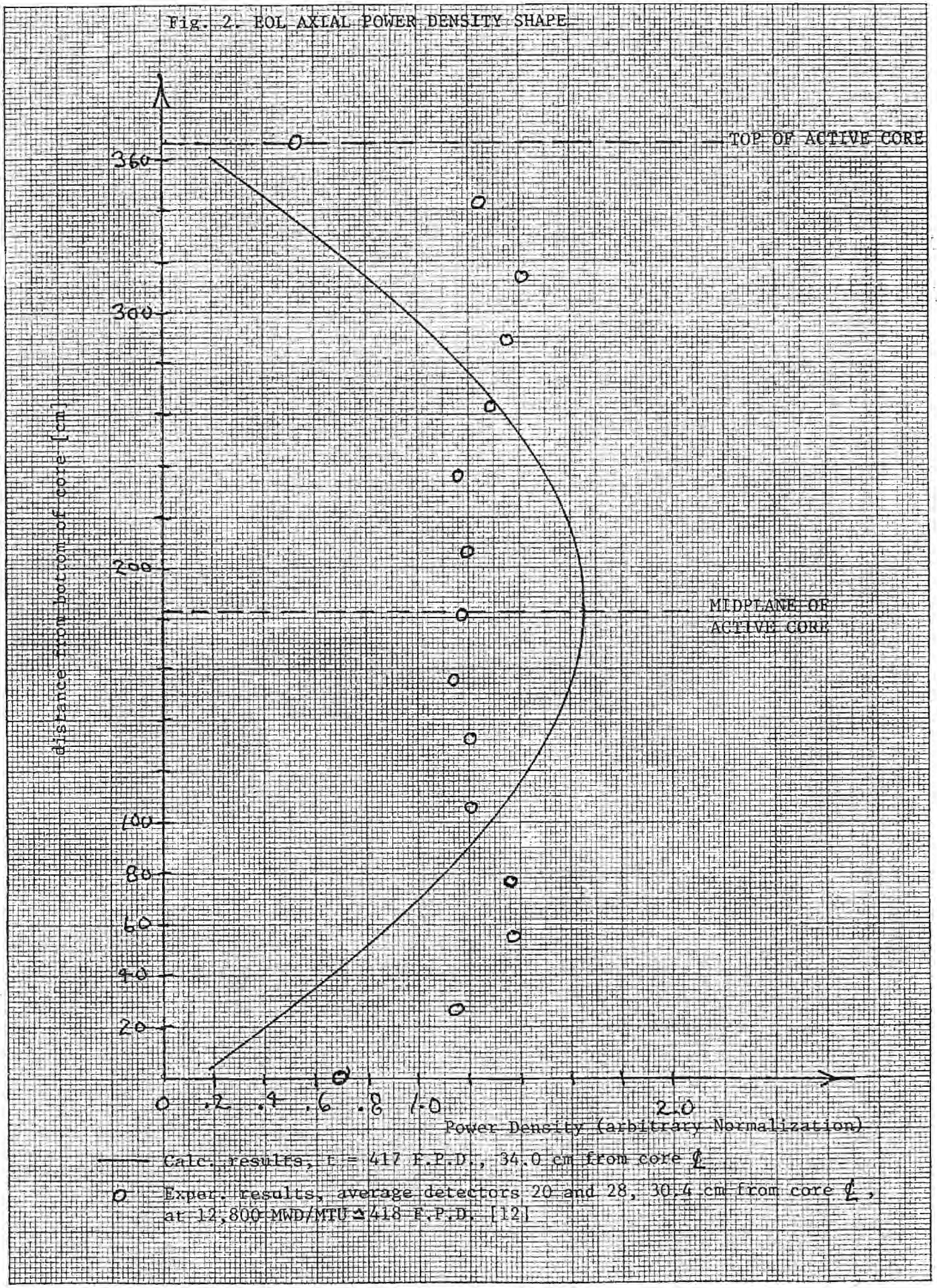

——— Calc. results, k_{eff} = 417 E.P.D., 34.0 cm from core ℄

o Exper. results, average detectors 20 and 28, 30.4 cm from core ℄, at 12,800 MWD/MTU ≙ 418 E.P.D. [12]

REFERENCES

[1] G. V. Neill and D. P. Johnson, "COROPT: A Computer Program for Finding Optimum LMFBR Mixed-Oxide Fuel Cores," GEFR-00006, UC-79B, General Electric Fast Breeder Reactor Department, Sunnyvale, California (January 1977).

[2] D. Rinaldis and J. M. Kallfelz, "Proposed Reactor Model for GE/ORNL/Ga Tech Studies of Impact of Design Data Uncertainties on Performance," Memorandum to: J. M. Marable and C. R. Weisbin, Georgia Institute of Technology, May 14, 1979.

[3] B. Talwar, Preconceptual Design of Proliferation Resistant, Homogeneous, Oxide-Fueled LMFBR Cores, General Electric Company Advanced Reactor Systems Department, Sunnyvale, California, August 1, 1978.

[4] "Final Report of the Proliferation Resistant Preconceptual Core Design Study, TC-1286," Hanford Engineering Development Laboratory, November 7, 1978.

[5] J. C. Chandler et al., "The Proliferation Resistant Preconceptual Core Design Study, TC-1082," Hanford Engineering Development Laboratory, March 1978.

[6] A Livrieri and J. M. Kallfelz, Private communication to C. R. Weisbin and J. R. Marable, dated March 30, 1979. Topic: Progress Report on COROPT work. . .., Period March 1-31, 1979.

[7] Ed Kujawski (GE-ARSD), private communication to J. M. Kallfelz, May 1979.

[8] C. R. Weisbin, J. M. Kallfelz, H. S. Bailey and E. Kujawski, "Economic Impact of Uncertainties in Data Adopted for Core Design," Attachment to letter from D. B. Trauger, Oak Ridge National Laboratory, to R. G. Staker, Department of Energy, with same subject as attachment, dated September 25, 1978.

[9] J. H. Marable and C. R. Weisbin, "Uncertainties in the Breeding Ratio of a Large LMFBR," Proceedings of the ANS Topical Meeting, Gatlinburg, Tennessee, April 10-12, 1978, CONF. 780401 [pg. 231-243].

[10] P. Greebler, B. A. Hutchins and R. B. Linford, "Significance of Neutron Data Uncertainties to Fast Reactor Economics and Power Plant Design," GEAP-5635, General Electric Co. (June 1968).

[11] Memo to C. R. Weisbin, J. H. Marable and M. L. Williams, from J. M. Kallfelz, D. Rinaldis and R. W. Carlson, "Progress Report for ORNL Subcontract 3986, Period April 1-30, 1979."

[12] "Reactor Core Physics Design and Operating Data for Cycles 1, 2, and 3 of the Turkey Point #3 PWR Power Plant," NP-827, Electric Power Research Institute, July 1978.

[13] D. A. Meneley, et al., "MACH 1, A One-Dimensional Diffusion Theory Package," ANL-7223, June 1966.

[14] H. C. Honeck, "Thermos, A Thermalization Transport Theory Code for Reactor Lattice Calculations," BNL-5826, September 1961.

[15] T. B. Fowler, et al., "Nuclaer Reactor Analysis Code: CITATION," ORNL-TM-2496, Rev. 2, July 1971.

SCHOOL OF NUCLEAR ENGINEERING

Atlanta, Georgia 30332

(404) 894-3720

July 8, 1979

MEMORANDUM

TO: C. R. Weisbin, J. H. Marable, and M. L. Williams (ORNL)

FROM: J. M. Kallfelz, D. Rinaldis, M. Segev, and P. Levin

SUBJECT: Progress Report on Work for ORNL Subcontract 3986, Period June 1 -30, 1979.

1. Summary

Our accomplishments this month are related to both sensitivity analysis and ARMP calculations.

o The calculations proposed in last month's progress report [1] to illustrate the influence of correlation between integral parameters on the variance of costs have been completed, and the resulting ANS summary is attached as Appendix A. This joint work involves the GE code COROPT and ORNL cross section sensitivity calculations. Further related considerations involving the k-reset mechanism are given in Appendix B.

o Methods employed in EPRI/CELL for the preparation and use of group cross sections have been investigated by M. Segev, and various observations and suggestions concerning these methods have been made.

o Our new co-worker, P. Levin, has familiarized himself with the calculational facilities available, and the CPM and EPRI/CELL code methods. He has initiated calculations of the BAPL-1, -2, and -3 lattices with EPRI/CELL.

Plans for next month's work are as follows:

o The major portion of the joint work involving COROPT and ORNL sensitivity calculations will be temporarily discontinued, awaiting decisions on the future of this program. A minor effort will continue regarding the k-reset considerations of Appendix B.

o Of the EPRI/CELL methods discussed in Section 2, it appears that the most promising topic for short-term investigations is related to area 2.5. Meir Segev plans to concentrate in his remaining time on this topic, namely a consistent definition of the σ_o parameter required for use of the f-factor tables.

o P. Levin's main priority will be to begin CPM calculations, and initiation of the code on the ORNL computer, once the necessary material is received from EPRI. On June 29 we were told by O. Ozer that he should be able to send some material in about a week, so we expect it soon. Until its arrival, P. Levin will perform calculations and analysis of the above-mentioned BAPL criticals.

2. Review of Cross Section Preparation Methods in EPRI/CELL (M. Segev)

Following are brief summaries of observations and suggestions relating to the methods employed in EPRI/CELL for the preparation and use of group cross sections.

Detailed discussions and/or derivation of formulae can be found in Reference 8 . A coherent and final section on the deviation of formulae and their implications will be attached to the next monthly report.

2.1 The Pin Absorption Cross Section

The pin absorption cross section is related to the resonance integral as follows

$$\sigma_{a,g} = \frac{\frac{I}{\Delta}}{1 - (1 + \lambda \frac{\Gamma_n}{\Gamma_\gamma}) \frac{I}{\Delta\sigma}}$$

where Δ is the group width (in lethargy) Γ_n and Γ_γ the neutron and capture widths of the resonance, λ the narrowness parameter of the resonance, and σ the background cross section ($\sigma_e + \sigma_{AM} + \lambda\sigma_{p,A}$).

The NAI prescription for $\sigma_a(I)$[2] neglects the second term in the denominator. This led to low values of σ_a, as evident in Table 6 of William's letter to Ozer, June 19, 1979.[3] An approximate correction to the NAI figures, based on the above formula, is

$$\sigma_{a,g} \simeq \frac{\sigma_{a,g}\ (NAI)}{1 - \frac{\sigma_{a,g}}{\sigma_o}\ (NAI)}$$

where σ_o is a σ entry in the cross section tables (such as Table 6 of William's, mentioned above). This correction brings the NAI values up so that they are more in line with other evaluations.[3,4]

2.2 Cell Averaging of Cross Sections

Presently no account is being taken of the fact that the average pin flux per cm^3 is depressed in comparison with the average moderator flux per cm^3; therefore, the cross sections that enter the P1 or B1* calculation are volume averages, not flux-volume averages.

In order to apply correct cross section values to the point diffusion calculation one must have a formula for the flux depression, namely a formula for the ratio $\phi_{fuel}/\phi_{moderator}$. Through discussions with Odelli Ozer and Bob McFarlane,[5] I found out that Bob derived an expression for ϕ_{fuel}/ϕ_{cell}:

$$\frac{\phi_{fuel}}{\phi_{cell}} = \frac{1}{1 + \left(\frac{\sigma_a}{\sigma_e + \lambda\sigma p\,fuel}\right)\ (1 - \beta)\ \frac{V_M}{V}}$$

---

*Ron Cobb pointed out that B-1 is the default (see input parameter PHITYP).

Table 2.1 Comparison of U238 Absorption Cross Sections

σ_o = 10, 300°

Group	NAI	NAI Corrected	Rolaids	LASL	ORNL NJOY
51	3.08	4.13	4.17	3.59	3.59
53	4.20	6.52	8.12	7.61	7.61
57	5.39	9.92	11.56	12.64	12.65

σ_o = 100, 300°

51	10.65	11.9	12.05	11.04
53	15.58	18.4	20.46	19.93
57	26.16	35.2	36.47	37.31

where

$$\beta = \frac{V_F \sigma_e}{V_M \sigma_M}$$

where σ_a is the group fuel absorption cross section, σ_e is the escape cross section and σ_M the moderator cross section.

This formula for the flux depression compares well with Rabble runs.[5] Furthermore the BAPL-1 k_{eff} is .969 without, and .987 with the application of the flux depression to EPRI/CELL cross sections.[5] The above formula is contained in a letter from McFarlane to Ozer of a few months ago, which Bob will send us.

2.3 On the Use of the Improved Removal Treatment

The macroscopic removal cross section is related to the escape probability and absorption cross section via

$$\Sigma_{R,g} = \Sigma_{a,g} \frac{X_g - 1 + P_g}{1 - P_g}$$

where $\Sigma_{R,g}$, $\Sigma_{a,g}$ are the removal and absorption group cross sections, P_g is the resonance escape probability for the group, and X_g is the fraction of neutrons entering the group out of the total number of neutrons that slow down past the top of the group.

In EPRI/CELL X_g is taken as 1.[2] This means that the IRT can be applied only for very large groups for which X(hydrogen) $\simeq$1. Presently the IRT is applied to the lowest fast group to provide slow-down from the fast library to the thermal library.[6] In this application there seems to be little error introduced by the assumption $X_g = 1$. However, due to the underestimation of $\Sigma_{a,g}$ by the NAI procedure (as explained in section 1 above), the $\Sigma_{R,g}$ will also be underestimated.

2.4 Interpolation of Self Shielding Factors

At a given temperature the F factor is very well represented by[7]

$$F(\sigma) = \sqrt{\frac{\sigma_p + \sigma}{\sigma_p + \sigma_{pk} + \sigma}}$$

for a large range of background σ values. In this formula σ_p and σ_{pk} are numerically determined parameters.

Applying the above formula as an interpolative means, σ_p and σ_{pk} are determined by two F-table entries, namely $F(\sigma_1)$ and $F(\sigma_2)$ or briefly F_1 and F_2. The interpolation formula which results is

$$F(\sigma) = \sqrt{\frac{F_1^2 (1 - F_2^2)\, \sigma_2 - F_2^2 (1 - F_1^2)\, \sigma_1 + (F_2^2 - F_1^2)\, \sigma}{(1 - F_2^2)\, \sigma_2 - (1 - F_1^2)\, \sigma_2 + (F_2^2 - F_1^2)\, \sigma}}$$

This formula should give very good results even in σ regions where $F(\sigma)$ is steep; and it removes the need to rely on mathematical devices for interpolating on a steep function, such as using the log of the function. A version of this latter device is currently implemented in EPRI/CELL.[2]

2.5 The Effect of Small Changes in Resonance Parameters on the Resonance Integral

Utilizing the functional form of the previous section for $F(\sigma)$ one can derive the following expression for the relative change in the resonance integral incurred by small changes in Γ_γ, Γ_n and σ -- respectively, the capture width, neutron width and total background cross section (including σ_p of absorber, σ_p of other elements and the escape cross section):

$$\frac{\delta I}{I} = \frac{1}{2}(1 - F^2)\left(\frac{\delta\sigma}{\sigma}\right) + \frac{\Gamma_\gamma}{\Gamma}\left[\frac{\Gamma_n}{\Gamma} + (1 - F^2)\left(1 - \frac{1}{2w_\lambda}\right)\right]\left(\frac{\delta\Gamma_\gamma}{\Gamma_\gamma}\right)$$
$$+ \frac{\Gamma_\gamma}{\Gamma}\left[1 - (1 - F^2)\left(1 - \frac{1}{2w_\lambda}\right)\right]\left(\frac{\delta\Gamma_n}{\Gamma_n}\right)$$

where $w_\lambda = \dfrac{\Gamma_\gamma + \lambda\Gamma_n}{\Gamma}$

The formula applies for a single resonance when changes in Γ_n and Γ_γ are considered. It can be applied to a group of resonances when a change in σ is considered.

There was an error in the first draft of this report[8] (copies to Williams, Weisbin, Kallfelz), in the coefficient of $(\delta\sigma/\sigma)$. The conclusion then drawn that the coefficient of $(\delta\sigma/\sigma)$ was extremely high for low F values was wrong.

The formula above takes into account changes in F induced by the changes in resonance parameters.

References

1. J. M. Kallfelz and D. Rinaldis, "Progress Report on Work for ORNL Subcontract 3986, Period 1 - 31 May, 1979," Memo to C. R. Weisbin, J. H. Marable, and M. L. Williams, dated June 6, 1979.
2. ARMP, Part II, Chapter 5, "EPRI-CELL Code Description," W. R. Cobb, W. J. Eich, D. E. Tivel (Oct. 1975).
3. M. Williams, "EPRI-CELL Calculations with LASL ENDF/B-IV Cross Sections," letter to O. Ozer (June 19, 1979).
4. M. Williams, private communications.
5. Telephone discussions with O. Ozer and R. McFarlane (July 2-5, 1979).
6. M. Williams and R. Cobb, private communications.
7. M. Segev, "A Theory of Resonance Group Self Shielding," Nucl. Sci. Eng. 56, p. 72 (1975).
8. M. Segev, handwritten first report on examination of EPRI-CELL methods, June 25, 1979.

Appendix A to ORNL Progress Report dated July 8, 1979

EVALUATION OF INTEGRAL PARAMETER CORRELATIONS AND REACTOR PERFORMANCE USING NUCLEAR DATA COVARIANCES

by

D. Rinaldis and J. M. Kallfelz (Georgia Tech),

E. Kujawski (GE-Sunnyvale),

and

J. H. Marable (ORNL)

A previous study[1] in our joint investigations illustrated the importance of considering the strong interplay of nuclear, mechanical, and thermal-hydraulic (T-H) aspects in assessment of reactor design. In this summary we discuss methods for utilizing covariance information to evaluate integral parameter correlations and the associated economic uncertainties.

We illustrate the impact of such correlations with an example which employs only nuclear data covariance files, but the method is meant to include non-nuclear data as well. Indeed, the inclusion of the latter has become more practical with the growth of data banks which contain information on uncertainties of T-H and mechanical properties[2] and the development of sensitivity theory for T-H problems.[3]

ENDF/B covariance matrices, [COV], contain information on both the standard deviation, SD, and correlation of various cross sections.[4] The use of [COV] to calculate SD for the breeding ratio, BR , and the multiplication constant, k, have been discussed in reference 5. For an integral parameter, I, e.g.. BR or k ,

$$\text{VAR}(I) = \sum_{i,j} \frac{\partial I}{\partial \sigma_i} \frac{\partial I}{\partial \sigma_j} \text{COV}(\sigma_i, \sigma_j) \qquad (1)$$

where the partial derivatives are sensitivity coefficients[5] and the variance, VAR, is SD^2.

This formalism can be extended to estimate the standard deviation of electricity cost using

$$\text{VAR}(\$) = \sum_{i,j} \frac{\partial \$}{\partial I_i} \frac{\partial \$}{\partial I_j} \text{COV}(I_i, I_j) \qquad (2)$$

where

$ = fuel cycle cost (or another reference value, such as core cost[1])

I_i = integral parameter i, and

$COV(I_i,I_j)$ = covariance matrix element describing the correlation between I_i and I_j. For i = j this element is SD^2.

If we consider only nuclear parameters,

$$COV\ (I_k,\ I_l) = \sum_{i,j} \frac{\partial I_k}{\partial \sigma_i} \frac{\partial I_l}{\partial \sigma_j}\ COV\ (\sigma_i,\ \sigma_j)\ . \qquad (3)$$

The cost sensitivity coefficients, $\partial \$ / \partial I_i$, can be calculated with COROPT[6] while the $COV(I_k,I_l)$ can be calculated with the methods described in references 5 and 7.

If one assumes no correlation, the [COV] matrix in Eqn. (2) has only diagonal terms, and

$$VAR\ (\$) = \sum_i \left[\frac{\partial \$}{\partial I_i}\ SD\ (I_i) \right]^2 \qquad (4)$$

Expression (4) is similar to the expression used in reference 8 to obtain the uncertainty ranges of fuel costs and various integral parameters, at a time when detailed covariance information for neutron cross sections was not available.

For the following example we limited the integral parameters to BR and the critical enrichment, ε , so the results of Eqn. (2) are not the true variance since not all significant integral parameters are included. Furthermore, the absolute values are influenced by uncertainties in the economic parameters we used (from the sample case in reference 6) and differences in methods used to determine the integral parameters in COROPT

and the codes used in reference 5. However, the difference between the results for the relative variance, VAR ($)/^{2}, from Eqns. (2) and (4), calculated in a consistent manner, is significant. It demonstrates the influence on the estimated cost uncertainties of considering the integral parameter correlation.

The reactor considered for this example is that described in the first problem issued by the Large Core Code Evaluation Working Group (LCCEWG).[9] The calculation of the integral parameter [COV] matrix of Eqn. (3) was accomplished with the cross section [COV] matrix and sensitivity coefficients available from the work reported in reference 5, while the cost sensitivity coefficients of Eqns. (2) and (4) were calculated with COROPT.[6] It should be noted that ENDF/B-IV covariance matrices were used, and the values of the cross section [COV] could be considerably different if adjusted cross section values[5] were used.

The integral data sensitivity coefficients $\partial I/\partial \sigma$ and cost sensitivity coefficients $\partial \$/\partial I$ used were consistent in that they were both true partial derivatives, with all other parameters fixed. Thus, the COROPT runs were sensitivity runs with no "reoptimization"[1,6] of the design after the integral parameter change, while the BR sensitivity coefficients used from reference 5 were those without an enrichment change for "k-reset". Note that the correlation between BR and the critical enrichment is included in Eqn. (2).

The COV (ε ,BR) matrix element was derived from that for COV (k,BR) using the calculated value $\frac{\varepsilon}{k}\frac{\partial k}{\partial \varepsilon} = -0.55$. (ε is the <u>critical</u> enrichment; hence the negative sign.)

Calculated values of interest are given in Table 1. The correlation coefficient, defined in the table footnote (B) of 0.89 indicates the strong correlation between BR and ε. As expected, considering this correlation reduces the relative variance of the fuel cycle cost appreciably, with an associated reduction in SD($). This demonstrates the importance of considering such correlations in evaluating the uncertainties in the economic performance of various reactor designs. As suggested in reference 1, such uncertainties may influence the decision process.

References

1. E. Kujawski, J. M. Kallfelz, and J. H. Marable, "Nuclear Uncertainties as a Consideration in Reactor Designs," Trans. Am. Nucl. Soc. 32, 791 (1979).

2. N. M. Greene et al., "SACRD: A Data Base for Fast Reactor Safety Computer Codes - General Description," ORNL-5477, Oak Ridge National Laboratory, (January 1979).

3. E. M. Oblow, "Sensitivity Theory for Reactor Thermal-Hydraulics Problems," Nucl. Sci. Engr. 68, 332 (1978).

4. F. G. Perey, G. de Saussure, and R. B. Perez, "Estimated Data Covariance Files of Evaluated Cross Sections - Examples for ^{235}U and ^{238}U," in Advanced Reactors: Physics, Design, and Economics, J. M. Kallfelz and R. A. Karam, Eds., Pergamon Press, Oxford and New York, p. 578 (1975).

5. J. H. Marable and C. R. Weisbin, "Uncertainties in the Breeding Ratio of a Large LMFBR," Proc. ANS Reactor Physics Division Topcial Meeting, Gatlinburg, Tennessee (April 1978).

6. G. V. Neill and D. P. Johnson, "COROPT: A Computer Program for Finding Optimum LMFBR Mixed-Oxide Fuel Cores," GEFR-00006, UC-798, General Electric Fast Breeder Reactor Department, Sunnyvale, California (January 1977).

7. C. R. Weisbin et al., "Applications of FORSS Sensitivity and Uncertainty Methodology to Fast Reactor Integral Experiment Analysis," Nucl. Sci. and Eng. 66, 307-333 (1978).

8. P. Greebler, B. A. Hutchins, and R. B. Linford, "Sensitivity of Fast Reactor Economics to Uncertainties in Nuclear Data," Nucl. Appl. 4, 297 (1968).

9. E. Kujawski and H. S. Bailey, "Benchmark Analysis of Liquid Metal Fast Breeder Reactor Nuclear Design Methods," Nucl. Sci. Eng. 64, 90-94 (September 1977).

TABLE 1 Some Calculated Results for an Example Considering Two Integral Parameters, BR and ε (see text) [a,b]. For These Values \$ is the Fuel Cycle Cost, 4.335 mills/kwh

Parameter	From Eqn. (2) (with correlation)	From Eqn. (4) (without correlation)
$\frac{VAR(\$)}{(\$)^2}$	3.41 -03	4.99 -03
$\frac{SD(\$)}{\$}$	5.84 -02	7.06 -02
SD(\$)	0.25 $\frac{mills}{kwh}$	0.31 $\frac{mills}{kwh}$

a. The following calcualted values were used to obtain the above results:

$$\frac{BR}{\$}\frac{\partial \$}{\partial BR} = -1.14; \quad \frac{\varepsilon}{\$}\frac{\partial \$}{\partial \varepsilon} = 0.35$$

$$[COV] = \begin{bmatrix} \frac{SD^2(\varepsilon)}{\varepsilon^2} & \frac{COV(BR,\varepsilon)}{BR \cdot \varepsilon} \\ \frac{COV(\varepsilon,BR)}{\varepsilon \cdot BR} & \frac{SD^2(BR)}{BR^2} \end{bmatrix} = \begin{bmatrix} 1.31\text{-}03 & 1.95\text{-}03 \\ 1.95\text{-}03 & 3.70\text{-}03 \end{bmatrix}$$

b. Note that $\frac{SD(\varepsilon)}{\varepsilon} = 3.6\%$, $\frac{SD(BR)}{BR} = 6.1\%$ and

$$\text{Correlation coefficient} = \frac{COV(\varepsilon, BR)}{SD(\varepsilon) \cdot SD(BR)} = 0.89$$

Appendix B to ORNL Progress Report dated July 8, 1979

Some Considerations on Explicitly Including a k-reset Mechanism in Evaluation of Integral Parameter Correlations and Reactor Cost Performance

The study discussed in Appendix A. used sensitivity coefficients which did not include a "k-reset" mechanism. As mentioned on page A3, the correlation between the breeding ratio (BR) and critical enrichment is included in the formalism used. The following comments are not meant to be complete, but to stimulate discussion on the covered topics.

B.1. General Comments

B.1.1. Independent and Dependent Variables

The k-reset mechanism is somewhat analogous to the question of independent and dependent variables for cross section sensitivity calculations [B1]. As discussed in ref. B1, a choice must be made between σ_t or one of the partial cross sections as a dependent variable. The most usual choice for the dependent variable in the high energy range has been σ_{el}, which in some sensitivity codes [B2] is changed when another partial σ is perturbed, to keep σ_t constant.

This suggests that in the example considered in Appendix A, one might assume only one independent variable, BR, with enrichment being a dependent variable adjusted to keep k constant. This led to the comparison of the two approaches in section B.2, below. However, this analogy should not be carried too far, for as discussed in the next section cross sections are independent input variables, while the integral parameters are functions thereof.

B.1.2. Independent Variables and Functions

While it may seem too obvious to mention, some care must be exercised in rewriting terms which involve quotients or products of partial derivatives. Equations (9) and (10) of [B1] give examples of the form $\frac{\partial \phi}{\partial x}$ and $\frac{\partial \phi}{\partial y}$, where $\phi = \phi(x,y) = \Phi(u,v)$, with $u = u(x,y)$ and $v = v(x,y)$.

In our case of interest, $\phi \triangleq \$$, $(u,v) \triangleq I_k$ and $(x,y) \triangleq \sigma_i$.

As an example, for the cost sensitivity coefficients $\partial \$/\partial BR$ a term "$\partial k/\partial BR$" would be analogous to the k-reset term in cross section sensitivities. However, since k and BR are different functions of the independent variables, such a term can not be defined. In some cases it may be sufficient to use ratios of derivatives with respect to some independent variable, i.e. $\frac{\partial k}{\partial \varepsilon} \Big/ \frac{\partial BR}{\partial \varepsilon}$, where in this appendix the enrichment and critical enrichment are designated by ε and ε_c, respectively. (Note that in Appendix A ε is the critical enrichment.)

As an example of the potential pitfalls, consider the following. In the development in Section B.2, terms appear of the form $\frac{\partial \$}{\partial \varepsilon_c} \Big/ \frac{\partial BR}{\partial \varepsilon_c}$. This can not be considered $\frac{\partial \$}{\partial BR}$, which is determined by the Pu gain term of the fuel cycle cost. $\frac{\partial \$}{\partial \varepsilon_c}$ is determined primarily by inventory charges.

This point can be illustrated numerically with the following values from Appendix A and reference 5 of that appendix.

$$\left[\frac{\frac{\varepsilon}{BR}\frac{\partial BR}{\partial \varepsilon}}{\frac{\varepsilon}{k}\frac{\partial k}{\partial \varepsilon}}\right] = -1.99; \quad \frac{\varepsilon}{k}\frac{\partial k}{\partial \varepsilon} = 0.55 \; ; \therefore \frac{\varepsilon}{BR}\frac{\partial BR}{\partial \varepsilon} = -1.09$$

Thus $\left(\frac{\varepsilon}{\$}\frac{\partial \$}{\partial \varepsilon}\right)\Big/\left(\frac{\varepsilon}{BR}\frac{\partial BR}{\partial \varepsilon}\right) = \underline{\underline{-0.32}}$ (B-1)

On the other hand, $\frac{BR}{\$}\frac{\partial \$}{\partial BR} = \underline{\underline{-1.14}}$ (B-2)

B.1.3. Numerical Differences in Var($) for the Different Approaches

The main contributor to VAR($) in Appendix A is the term involving the $\frac{SD(BR)}{BR}$ =6.1%. For SD of the breeding ratio involving k-reset, $SD_r(BR)$, this value is much lower, namely 3.12%, as reported in ref. 5 of Appendix A.

Furthermore, one would expect the cost coefficient accounting for k-reset enrichment changes $\left(\frac{\partial \$}{\partial BR}\Big|_r\right)$ to be smaller than $\frac{\partial \$}{\partial BR}$. If BR increases, $ decreases due to increased Pu gain. But due to the correlation between BR and ε_c, one would expect ε_c to also increase, tending to increase $.

The proper definition of $\frac{\partial \$}{\partial BR}\Big|_r$ is not clear to the author, and needs more consideration. As discussed in section B.2, the cost coefficients associated with k-reset mechanisms can be defined more easily when costs coefficients are defined for individual cross sections, as in eqn (5) of [B3]. However, the following definition seems plausible, and serves to illustrate the reduction in $\frac{\partial \$}{\partial BR}\Big|_r$.

Assume $\frac{\partial \$}{\partial BR}\Big|_r = \frac{\partial \$}{\partial BR} - a\left(\frac{\partial k}{\partial \varepsilon}\right)\Big/\left(\frac{\partial BR}{\partial \varepsilon}\right)$ (B-3)

where $a = \left(\frac{\partial \$}{\partial \varepsilon}\right)\Big/\left(\frac{\partial k}{\partial \varepsilon}\right)$

Thus

$$\frac{\partial \$}{\partial BR}\Big|_r = \frac{\partial \$}{\partial BR} - \left(\frac{\partial \$}{\partial \varepsilon}\right)\Big/\left(\frac{\partial BR}{\partial \varepsilon}\right) \quad (B-4)$$

Or, using values given in section B.1.2,

$$\frac{BR}{\$}\left.\frac{\partial \$}{\partial BR}\right|_r = -1.14 + 0.32 = -0.82 \qquad (B\text{-}5)$$

Then, if we assume that for the case in Appendix A there is only one independent variable, BR, with k-reset effects included in the sensitivity coefficients:

$$\frac{VAR(\$)}{\$^2} = \left(\left.\frac{\partial \$}{\partial BR}\right|_r\right)^2 \frac{SD_r^2(BR)}{BR^2}$$

$$= (-0.82)^2(0.0312)^2 = \underline{\underline{6.55-4}} \qquad (B\text{-}6)$$

This value is considerably lower than the values in Appendix A. In the following section we will analytically examine the difference in the expressions for the VAR($).

B.2 Analytic Examination of Expressions With and Without Explicit k-reset Term

In this section we will write and compare the analytic expressions for VAR($) for two cases:

Case 1. Two independent (but correlated) integral variables, and BR.

Case 2. One independent variable, BR, but with "k-reset" in the sensitivity coefficients.

We convert $\frac{1}{k \cdot BR}\,COV(k,BR)$ to $\frac{1}{\varepsilon_c \cdot BR}\,COV(\varepsilon_c, BR)$ as described in Appendix A, by multiplying the former by

$$\left[-\frac{\varepsilon}{k}\frac{\partial k}{\partial \varepsilon}\right]^{-1} = \left[-0.55\right]^{-1} = -1.82 \qquad \text{(B-7)}$$

It is conceptually preferable to define this conversion factor as

$$\frac{k}{\varepsilon_c}\frac{\partial \varepsilon_c}{\partial k} = -1.82 \qquad \text{(B-8)}$$

Thus we have assumed that k changes are compensated with enrichment.

Furthermore, while we speak of critical enrichment for this example, the same formalism holds for a BOL k, slightly greater than 1.0 to allow for the cycle Δk.

B.2.1. Two Independent (but Correlated) Variables

Considering first Case 1, we use the same expression as in Appendix A:

$$VAR(\$) = \left(\frac{\partial \$}{\partial BR}\right)^2 SD^2(BR) + \left(\frac{\partial \$}{\partial \varepsilon_c}\right)^2 SD^2(\varepsilon_c) + 2\,\frac{\partial \$}{\partial BR}\,\frac{\partial \$}{\partial \varepsilon_c}\,COV(\varepsilon_c, BR) \qquad \text{(B-9)}$$

B.2.2. One Independent Variable with "k-reset" Effect in Integral Parameter Sensitivity Coefficients

Considering Case 2:

$$VAR_r(\phi) = \left(\frac{\partial \phi}{\partial BR}\Big|_r\right)^2 SD_r^2(BR) \tag{B-10}$$

$$SD_r^2(BR) = COV_r(BR, BR)$$

$$= \sum_{i,j}{}' \left(\frac{\partial BR}{\partial \sigma_i} - \frac{\partial k}{\partial \sigma_i} b\right)\left(\frac{\partial BR}{\partial \sigma_j} - \frac{\partial k}{\partial \sigma_j}\right) COV(\sigma_i, \sigma_j) \tag{B-11}$$

where $b = \left[\frac{\partial BR}{\partial \epsilon} \Big/ \frac{\partial k}{\partial \epsilon}\right]$. (B-11a)

(See ref. 5 of Appendix A.)

Rewriting terms in eqn. (B-11),

$$SD_r^2(BR) = \sum_{i,j}{}' \left\{ \frac{\partial BR}{\partial \sigma_i}\frac{\partial BR}{\partial \sigma_j} + \frac{\partial k}{\partial \sigma_i}\frac{\partial k}{\partial \sigma_j} b^2 - b\left[\frac{\partial k}{\partial \sigma_i}\frac{\partial BR}{\partial \sigma_j} + \frac{\partial k}{\partial \sigma_j}\frac{\partial BR}{\partial \sigma_i}\right] COV(\sigma_i, \sigma_j)\right\} \tag{B-12}$$

$$\sum_{i,j} b\left[\text{in B-12}\right] = 2b \sum_{i,j} \frac{\partial k}{\partial \sigma_i}\frac{\partial BR}{\partial \sigma_j} COV(\sigma_i, \sigma_j) \tag{B-13}$$

Thus, from eqns. (B-12) and (B-13):

$$SD_r^2(BR) = SD^2(BR) + b^2 SD^2(k) - 2b\, COV(BR, k) \tag{B-14}$$

$$COV(BR, \epsilon_c) = COV(BR, k)\frac{d\epsilon_c}{dk} \tag{B-15}$$

Therefore

$$SD_r^2(BR) = SD^2(BR) + c^2 SD^2(\epsilon_c) - 2c\, COV(BR, \epsilon_c) \tag{B-16}$$

where $c = \dfrac{b}{d\epsilon_c/dk} = -\dfrac{\partial BR}{\partial \epsilon}$ (B-17)

considering that $\dfrac{d\epsilon_c}{dk} = -1 \Big/ \dfrac{\partial k}{\partial \epsilon}$.

Equation (B-16) is interesting, in that one sees the same factors present as for Case 1. in eqn. (B-9), i.e. SD^2 of BR and ε_c, as well as COV(BR, ε_c).

As a matter of interest, it appeared during our initial investigations that using eqn. (B-16) in eqn. (B-10), but with $\frac{\partial \$}{\partial BR}$ <u>without</u> a k-reset term instead of $\frac{\partial \$}{\partial BR}\Big|_r$ in eqn. (B-10) yielded the same result for $VAR_r(\$)$ as did eqn. (B-9), which is for case 1. However, this result was proved later to be wrong, caused by errors in rewriting terms involving products and quotients of derivatives (reference sec. B.1.2.).

Continuing with the development of eqn. (B-10), we now need to define $\frac{\partial \$}{\partial BR}\Big|_r$. The problem in defining this term has been discussed in sec. B.1.3., and we will make the same assumption as was made there (eqn. B-4), i.e.

$$\frac{\partial \$}{\partial BR}\Big|_r = \frac{\partial \$}{\partial BR} - \left(\frac{\partial \$}{\partial \varepsilon_c} \Big/ \frac{\partial BR}{\partial \varepsilon_c}\right) \qquad \text{(B-18)}$$

since $\frac{\partial \$}{\partial \varepsilon} = \frac{\partial \$}{\partial \varepsilon_c}$ and $\frac{\partial BR}{\partial \varepsilon} = \frac{\partial BR}{\partial \varepsilon_c}$.

$$\therefore \left(\frac{\partial \$}{\partial BR}\Big|_r\right)^2 = \left(\frac{\partial \$}{\partial BR}\right)^2 + \frac{1}{c^2}\left(\frac{\partial \$}{\partial \varepsilon_c}\right)^2 + \frac{2}{c}\frac{\partial \$}{\partial BR}\frac{\partial \$}{\partial \varepsilon_c} \qquad \text{(B-19)}$$

using eqns. (B-16) and (B-19) in (B-9):

$$VAR_r(\$) = \underset{(A)}{SD^2(BR)\left(\frac{\partial \$}{\partial BR}\right)^2} + \underset{(B)}{SD^2(\varepsilon_c)\left(\frac{\partial \$}{\partial \varepsilon_c}\right)^2} - \underset{(C)}{4\frac{\partial \$}{\partial BR}\frac{\partial \$}{\partial \varepsilon_c}COV(BR, \varepsilon_c)}$$

$$+ SD^2(BR)\left[\frac{1}{c^2}\left(\frac{\partial \$}{\partial \varepsilon_c}\right)^2 + \frac{2}{c}\frac{\partial \$}{\partial BR}\frac{\partial \$}{\partial \varepsilon_c}\right]$$

$$+ c^2 SD^2(\varepsilon_c)\left[\left(\frac{\partial \$}{\partial BR}\right)^2 + \frac{2}{c}\frac{\partial \$}{\partial BR}\frac{\partial \$}{\partial \varepsilon_c}\right]$$

$$- 2c\left[\left(\frac{\partial \$}{\partial BR}\right)^2 + \frac{1}{c^2}\left(\frac{\partial \$}{\partial \varepsilon_c}\right)^2\right] COV(BR, \varepsilon_c) \qquad \text{(B-20)}$$

Examining eqn. (B-20) shows many terms similar to those for Case 1, eqn. (B-9). In particular, terms (A) + (B) + (C) are the same as eqn. (B-9), except for the -4 in (C). Unfortunately, however, our efforts to rewrite eqn. (B-20) in some simpler form, either equivalent to eqn. (B-9), or with differences which can be easily explained, have thus far been unsuccessful. Considering the possibility that the definition in eqns. (B-4) and (B-18) is not correct, we thus define the cost coefficients for the individual cross sections in the following section.

B.2.3. One Independent Variable, with "k-reset" Mechanism in Cost Coefficients for Individual Cross Sections

A further approach to compare cases 1 and 2 would be to use the cross sections as the basic parameters, rather than the integral parameters. For this approach the cost sensitivity associated with the k-reset mechanism is perhaps easier to define, since it can be associated with each σ_i .

Thus, the basic equation to use is that of eqn. (5) of ref. [B3]:

$$VAR(\$) = \sum_{i,j} \frac{\partial \$}{\partial \sigma_i} \frac{\partial \$}{\partial \sigma_j} COV(\sigma_i, \sigma_j) \qquad \text{(B-21)}$$

To show that this is the equivalent of eqn. (2), Appendix A, we note that eqn. (12) of ref. [B3] in its full form is:

$$\frac{\partial \$}{\partial \sigma_i} = \sum_k \frac{\partial \$}{\partial I_k} \frac{\partial I_k}{\partial \sigma_i} \qquad \text{(B-22)}$$

Thus eqn. (B-21) becomes

$$VAR(\$) = \sum_{i,j} \left[\sum_k \frac{\partial \$}{\partial I_k} \frac{\partial I_k}{\partial \sigma_i} \right] \left[\sum_l \frac{\partial \$}{\partial I_l} \frac{\partial I_l}{\partial \sigma_j} \right] \cdot \qquad \text{(B-23)}$$

$$\cdot COV(\sigma_i, \sigma_j)$$

Changing the order of summation

$$VAR(\not\$) = \sum_{k,l} \frac{\partial \not\$}{\partial \bar{I}_k} \frac{\partial \not\$}{\partial \bar{I}_l} \sum_{i,j} \frac{\partial I_k}{\partial \sigma_i} \frac{\partial \bar{I}_l}{\partial \sigma_j} COV(\sigma_i, \sigma_j) \tag{B-24}$$

As defined in eqn. (3) of Appendix A, the second summation in eqn. (B-24) is $COV(I_k, I_l)$. Thus eqn. (B-24) becomes

$$VAR(\not\$) = \sum_{k,l}' \frac{\partial \not\$}{\partial \bar{I}_k} \frac{\partial \not\$}{\partial \bar{I}_l} COV(\bar{I}_k, \bar{I}_l) \tag{B-25}$$

which is identical to eqn. (2) of Appendix A.

Returning to the problem of writing eqn. (B-21) with k-reset mechanism included, we face the problem of defining $\frac{\partial \not\$}{\partial \sigma_i}\Big|_r$, including the k-reset effect. If we assume only one independent variable, BR, with k-reset (see ref. 5, Appendix A):

$$\frac{\partial BR}{\partial \sigma_i}\Big|_r = \frac{\partial BR}{\partial \sigma_i} - \frac{\partial k}{\partial \sigma_i} b \tag{B-26}$$

where b is defined in eqn (B-11a).

Then: $$\frac{\partial \not\$}{\partial \sigma_i}\Big|_r = \frac{\partial BR}{\partial \sigma_i}\Big|_r \frac{\partial \not\$}{\partial BR} - \frac{\partial k}{\partial \sigma_i} e \tag{B-27}$$

where $e = \frac{\partial \not\$}{\partial \varepsilon} \Big/ \frac{\partial k}{\partial \varepsilon}$ (B-28)

If we assume that

$$\frac{\partial k}{\partial \sigma_i} \Big/ \frac{\partial k}{\partial \varepsilon} = - \frac{\partial \varepsilon_c}{\partial \sigma_i} \tag{B-29}$$

then eqn. (B-27) can be rewritten as

$$\frac{\partial \not\$}{\partial \sigma_i}\Big|_r = \left(\frac{\partial BR}{\partial \sigma_i} + \frac{\partial \varepsilon_c}{\partial \sigma_i} \frac{\partial BR}{\partial \varepsilon_c} \right) \frac{\partial \not\$}{\partial BR} + \frac{\partial \varepsilon_c}{\partial \sigma_i} \frac{\partial \not\$}{\partial \varepsilon_c} \tag{B-30}$$

$$\frac{\partial \not\$}{\partial \sigma_i}\Big|_r = \left\{ \underbrace{\frac{\partial BR}{\partial \sigma_i} \frac{\partial \not\$}{\partial BR}}_{(A)} + \underbrace{\frac{\partial \varepsilon_c}{\partial \sigma_i} \frac{\partial \not\$}{\partial \varepsilon_c}}_{(B)} + \underbrace{\frac{\partial \varepsilon_c}{\partial \sigma_i} \frac{\partial BR}{\partial \varepsilon_c} \frac{\partial \not\$}{\partial BR}}_{(C)} \right\} \tag{B-31}$$

If we now use this expression in eqn (B-21), we get

$$VAR_r(\$) = \sum_{i,j} \left\{ \text{in B-31} \right\}_i \left\{ \text{in B-31} \right\}_j \; COV(\sigma_i, \sigma_j) \qquad \text{(B-32)}$$

We note that for case 1, with two independent but correlated variables, BR and ε_c, using eqn. (B-23):

$$VAR(\$) = \sum_{i,j} \left[\underbrace{\frac{\partial BR}{\partial \sigma_i} \frac{\partial \$}{\partial BR}}_{(A)} + \underbrace{\frac{\partial \varepsilon_c}{\partial \sigma_i} \frac{\partial \$}{\partial \varepsilon_c}}_{(B)} \right] [\cdots]_j \; COV(\sigma_i, \sigma_j) \qquad \text{(B-33)}$$

Comparing eqns. (B-32) and (B-33), we see that while the expression for Case 2 (B-31), contains all the terms of Case 1, i.e. terms (A) and (B), it also contains an extra term (C), which appears in many cross-products in eqn. (B-32). As is done for eqns. (B-21) through (B-25), terms in eqn. (B-32) involving (A) and (B) alone could be rewritten as functions of the integral parameters I_k and I_l. However, terms involving (C) still remain only for case 2, and until now our efforts to rewrite eqn. (B-32) have not resulted in a form which provides a simple physical explanation for the difference in the results for Cases 1 and 2.

Appendix B Reference

[B1] J.M. Kallfelz, Memo to F.C. Maienschein, "Status Report for the Georgia Institute of Technology Project E-26-610," March 19, 1975.

[B2] P.C.E. Hemment, et.al., "The Multigroup Neutron Transport Perturbation Program DUNDEE," AWRE O-40/66, UKAEA Aldermaston, October 1966.

[B3] C.R. Weisbin, J.M. Kallfelz, H.S. Bailey and E. Kujawski, "Economic Impact of Uncertainties in Data Adopted for Core Design," Attachment 1 to letter from D.B. Trauger, ORNL, to R.G. Staker, DOE, dated September 25, 1978.

SCHOOL OF NUCLEAR ENGINEERING

Atlanta, Georgia 30332 (404) 894–3720

E-26-1001
645

August 1, 1979

MEMORANDUM

TO: C. R. Weisbin and M. L. Williams (ORNL)

FROM: J. M. Kallfelz, P. Levin, and M. Segev

SUBJECT: Progress Report on Work for ORNL Subcontract 3986, Period July 1 - 31, 1979

1. Summary

1.1 Accomplishments for Report Period

- o EPRI-CELL calculations for BAPL-1, -2, and -3 assemblies have been accomplished, using both the NAI [2] and transport-corrected ENDF/B-IV [3] libraries. The input prepared can be used for repeat runs when modifications presently being incorporated in EPRI-CELL at ORNL are completed. An analysis of the present results has contributed to the understanding of the code and benchmarks, and has revealed some apparent discrepancies in the code which must be resolved.
- o A sample CPM run provided by Odelli Ozer was successfully executed on the Berkeley CDC 7600. The results and program description are presently being studied, to prepare for the task of initiating CPM on the ORNL IBM-360.
- o A review has been performed of cross section preparation methods in EPRI-CELL. The results of this review have been reported in ref. [4].

- o Information has been gathered concerning the use of the entire ARMP package at various sites. Based on our inquiries, use of the version operating on the BNL CDC 7600 appears attractive.

1.2 Plans for Next Month's Work

- o EPRI-CELL calculations will be performed for mixed oxide criticals [10,11] and isotopics of PWRs [12-14]. When the modifications presently being incorporated into the ORNL version of EPRI-CELL are completed, these calculations and those for the BAPL-1 through -3 uranium oxide assemblies will be repeated and analyzed.
- o Calculations with the Berkeley version of CPM will be continued, beginning with a BAPL-1 cell for comparison with EPRI-CELL and other CPM calculations [5]. As soon as the CPM FORTRAN source arrives from EPRI, work will begin on initiating this code on the ORNL IBM-360.
- o Related to the initiating and testing of CPM, we will start work on the development of an interface between NJOY [6] output and CPM input, because of a difference in the f-factor tabulations for the two codes.
- o We will continue our investigations concerning the most practical location to perform a complete reactor calculation using the entire ARMP package. If the associated administrative problems can be resolved this month, we will initiate such a calculation, similar to that performed at BNL [15].

2. EPRI-CELL Calculations

2.1 BAPL Models and Integral Parameter Results

EPRI-CELL calculations were performed on the ORNL IBM-360, using both the NAI [2] and transport-corrected ENDF/B-IV [3] libraries. Since modifications to EPRI-CELL have been initiated at ORNL after we started this series of calculations they will have to be repeated when the modifications are complete. Nonetheless, an analysis of the present results contributes to an understanding of the code and benchmarks, and the prepared input can be used for the reruns.

The results reported in this section are all from runs performed before July 20, when code modifications were initiated to incorporate McFarlane's correction for flux-volume weighting of the GAM cross sections [4].

The models used, described in Table 1, are from [7]. The lattices are triangular, and the outer radius of the equivalent cylindrical cell was calculated using

$$R_{cell} = \sqrt{\frac{\sqrt{3}}{2\pi}} \cdot P$$

where P is the pitch. The Dancoff correction was calculated using Sauer's approximation [8] with $\Sigma_t = 1.49$ cm^{-1}. The resulting Dancoff corrections are 0.2688, 0.2172, and 0.1586 for BAPL-1, -2, and -3 respectively.

The BAPL-1 code input was adapted from MacFarlane [9]. To be consistent with his results, the 0.02 cm void was replaced by clad; this results in an atom density 5.6% larger than for a smeared density considering the volume ratios of the clad and vacuum. Furthermore, his oxygen density input is slightly in error in the moderator region (.0338 should be .03338) but this should have a negligible effect on the calculation.

Since the spatial mesh used by MacFarlane and for our calculations seemed rather coarse, the least dense case, BAPL-3, was repeated with a spatial mesh four times finer. The changes in the results were negligible, the fine mesh case giving results differing from the original mesh by +0.04%, - 0.2%, and - 0.09% for k_{eff}, δ_{25}, and ρ_{28}, respectively.

The results for the original mesh are given in Table 2. For the NAI cross sections, our BAPL-1 results compare excellently with those of MacFarlane, run at LASL [9]. Since our calculations were performed before the above-mentioned code modifications were initiated at ORNL, this presumably means that for MacFarlane's NAI results reported in [9], this correction had also not yet been applied. It is not clear why MacFarlane's ENDF/B results for k_{eff} of BAPL-1 in [9] do not agree with the lower values reported in [4] and [16], particularly since Williams shows in [16] that the transport correction has negligible effect on this value. Possibly MacFarlane was in the process of initiating his correction to EPRI-CELL at the time, and has since made improvements there too.

The other results are of general interest, e.g. the NAI results for k_{eff} are good for all assemblies, while those for ENDF/B are all 2 - 3% lower. It is expected [4] that the flux-volume correction for GAM will improve the ENDF/B values, but it is not clear why the same corrections are not necessary for the NAI case. For the other results, the largest deviations between calculation (C) and experiment (E) are those for ENDF/B ρ_{28}, with (C-E)/E values of + 15% - 20%. The influence of the MacFarlane correction on these values remains to be seen, but presumably the reduction in the U^{238} σ_c values for groups with large resonances will be the most noticeable effect of the correction, thus improving the (C-E)/E results.

2.2. EPRI-CELL Result Discrepancies for Same Supercell Case, but Different Edit Cell

A BAPL-1 case was run with only the edit cell changed from the supercell to fuel only. The following inexplicable changes occurred in the GAM macroscopic cross sections:

(a) The Σ_a upper 4 group values are higher by up to 1% for the fuel edit.

(b) The Σ_t values for the upper 10 groups are higher by 2 - 3% for the fuel edit.

Furthermore, the resulting fast flux is reduced by 2 - 3% in the groups with the highest flux values (6 - 10) for the final edit case. Due to normalization the remaining fast and thermal flux values are about 0.2% higher for this case, while the two group supercell k_{eff} increases by 0.1%. Similar discrepancies were observed for the NAI cross sections, and for both sigma sets these cross section discrepancies for the above mentioned high groups were identical for runs before and after the initiation of code modifications on July 20.

We have a similar set of cases run on the Berkeley computer which does not exhibit the above discrepancies. This apparently indicates that the above-discrepancies are an error in the ORNL version, independent of the present modifications being made. While the effect is not large for the case considered, the results suggest the possibility of variable overflow into other data memory because of inadequate dimensions, and the problem should at any rate be resolved.

2.3. Differences Observed After Initiation of EPRI-CELL Modifications

Since the modification to EPRI-CELL to incorporate the MacFarlane flux-volume weighting correction for GAM are not yet complete, this section gives results observed so far merely to raise several questions.

As an example, BAPL-1 was run on July 24. As expected the modification to that date influenced the GAM sigma values, with both absorption and fission cross sections below group 25 (below 24.8 kev) being changed from a July 12 calculation. For ENDF/B, the new run had increases of up to 8% in Σ_a, and 130% for Σ_f, in the resonant groups, e.g. 51, 53, 57. Results for NAI sigma had the same trends, but the observed changes were much smaller, and start at a lower energy (group 48). This raises several questions:

(a) Why does the correction raise Σ_a and Σ_f? It appears physically that these values should be lowered, because of flux depression in the pin.

(b) Why are the changes so much greater for ENDF/B than for NAI?

3. Information Concerning Usage of the ARMP Package

The following information was obtained through discussions with Burt Zolotar and Odelli Ozer at EPRI, Dave Diamond at BNL, and various Georgia Tech computer staff members.

3.1 Sites Where We Can Use ARMP

There are three sites available for DOE users of ARMP, namely Berkeley, ANL and BNL. Burt Zolotar said that the ARMP package was sent to DOE, and they are assigning responsibility for initiation.

At Berkeley, Burt is only sure that EPRI-CELL, CPM, and PDQ are working. The former two codes were initiated by EPRI, while Burt believes Ron Omberg at HEDL has responsibility for initiation of the entire package. The exact status is not yet known, since I have not yet reached Ron.

At BNL, the entire package is running, and Dave Diamond's group has done an entire reactor case similar to that which we wish to perform [15]. Dave has given me the names of two staff members who use the code and the individual responsible for maintaining it, all of whom we could contact for advise when needed. Also, he says their CDC-7600 is simple to access remotely, and uses the standard CDC system.

At Georgia Tech we could access ARMP on CDC's CYBERNET, since we have a CYBER-74 computer. ARMP is available without royalty cost to all CYBERNET users. However, we would have to pay commercial computer use rates, which would be much more expensive than using DOE computers. This option might be attractive for a "one-time" test calculation.

Presently, it appears that BNL is the most attractive site for our purposes, but we are examining this question furter.

3.2. Comments on ARMP Usage

Burt Zolotar says that a simple ARMP user's handbook, treating practical questions of modeling, etc., should be distributed next week, along with a PDQ manual which is specifically for the ARMP version. We should try to get these documents promptly.

Regarding SIMULATE, which is presently being considered as a tool for your optimization program at ORNL, Burt says SIMULATE should supplement EPRI-NODE-B and -P, rather than replace them. He anticipates that companies will continue to use EPRI-NODE for scoping calculations. For PWR's, they have not yet used SIMULATE. For BWR's, they run CPM and edit an output file to generate cross sections for SIMULATE.

For PWR's, he believes that utilities will continue to use EPRI-CELL and PDQ, so they periodically use them for pin-by-pin calculations for ¼ core, to get very accurate results. Therefore, Burt believes that individual assembly PDQ calculations will probably be used to generate PWR cross sections for SIMULATE, by way of modified versions of EPRI-FIT and SUPERLINK-P. The necessary modifications to the latter codes have not yet been made.

Table 1. Models for BAPL-1, -2, and -3. All values except the moderator outer radii are from Ref 6. The lattices are triangular.

A. Common Characteristics (cylindrical geometry)

Region	Outer Radius (cm)	Isotope	Concentration (10^{24} atoms/cm^3)
Fuel	.4864	^{235}U	3.112×10^{-4}
		^{238}U	2.3127×10^{-2}
		O	4.6946×10^{-2}
Void	.5042	--	--
Clad	.5753	Al	6.025×10^{-2}
Moderator	(see B.)	O	3.338×10^{-2}
		H	6.676×10^{-2}

B. Individual Characteristics

Assembly	Triangular Pitch (cm)	Moderator outer radius (cm)	Total B^2 [m^{-2}]*
BAPL-1	1.5578	0.8179	32.59
BAPL-2	1.6523	0.8675	35.47
BAPL-3	1.8057	0.9481	34.22

*Values given are those used in our calculation. Ref. 5 gives their uncertainty as 0.15, 0.18, and 0.13 for BAPL-1, -2, and -3, respectively.

Table 2. Some results for BAPL critical assemblies. Calculated results are for the ORNL EPRI-CELL version prior to initiation of modifications of 20 July, with the exception of McFarlane's results from Ref. 9[a]. (C-E)/E values are given in square brackets.

Parameter	Source	BAPL-1		BAPL-2	BAPL-3
		Ref. 9[a]			
keff	NAI	.9998	.9984	.9989	.9980
"	ENDF	1.0025	.9713	.9759	.9797
δ_{25}[b]	EXP	.085	(±2.4%)	.068(±1.5%)	.052(±1.9%)
"	NAI	.0810	.0810	.0662	.0510
"	"	[-4.8%]	[-4.8%]	[-2.6%]	[-1.3%]
"	ENDF	.0809	.0807	.0659	.0507
"	"	[-4.8%]	[-5%]	[-3.1%]	[-2.5%]
ρ_{28}[b]	EXP	1.39	(±0.7%)	1.12(±0.9%)	.906(±1.1%)
"	NAI	1.353	1.353	1.130	.891
"	"	[-2.7%]	[-2.7%]	[+0.9%]	[-1.6%]
"	ENDF	1.371	1.597	1.334	1.053
"	"	[-1.4%]	[+14.9%]	[+19.1%]	[+16.2%]

a. Ref. 9 values without transport correction for ENDF

b. δ_{25} and ρ_{28} are the ratio of epithermal to thermal reactions for U-235 fission and U-238 capture, respectively.

References

1. "Advanced Recycle Methodology Program System Documentation," EPRI Report,CCM-3, Electric Power Research Institute, September 1977.

2. See Chapter 2, part II, of Ref. 1. The NAI generated EPRI-CELL libraries existing at ORNL were used: GAM library (FTO3) - Tape #X14156 THERMOS library (FTO4) - Tape #X03618

3. ENDF/B-IV - Based transport corrected EPRI-CELL libraries existing at ORNL were used: GAM library (FTO3) - Tape #X05013 THERMOS library (FTO4) - Tape X20252

4. M. Segev, "Review of Cross Section Preparation Methods in EPRI-CELL," Memorandum to J. M. Kallfelz, C. R. Weisbin, and M. L. Williams, July 20, 1979.

5. Sec. 3, Chapter 5, part I of Ref. 1.

6. R. E. MacFarlane et al., "The NJOY Nuclear Data Processing System: User's Manual," LASL Report LA-7584-M (ENDF-272) 1978.

7. H. Alter et al., "Cross Section Evaluation Working Group Benchmark Specifications," BNL-19302 (ENDF-202), Brookhaven National Laboratory, Revised September, 1978. Pages T(18-20)-1 to -3.

8. A. Sauer, "Approximate Escape Probabilities," Nucl. Sci. Eng. 16, 329 (1963).

9. R. E. MacFarlane (LASL), memo to O. Ozer (EPRI) "Thermal Transport and Removal Cross Sections in EPRI-CELL," April 18, 1979.

10. R. I. Smith and G. J. Konzek, "Clean Critical Experiment Benchmarks for Plutonium Recycle in LWRs," EPRI NP-196, Electric Power Research Institute, April 1976.

11. R. Sher and S. Fiarman, "Analysis of Some Uranium Oxide and Mixed-Oxide Lattice Measurements," EPRI NP-691, Electric Power Research Institute, Feb. 1978.

12. R. J. Nodvik et al., "Supplementary Report on Evaluation of Mass Spectrometric and Radiochemical Analyses of Yankee Core I Spent Fuel, Including Isotopes of the Elements Thorium through Curium," WCAP-6086 (Sept. 1969).

13. J. B. Melehan, "Yankee Core Evaluation Program, Final Report," WCAP-3017-6094 (January 1971).

14. R. J. Nodvik, "Saxton Core II Fuel Performance Evaluation Part II, Evaluation of Mass Spectrometric and Radiochemical Analysis of Irradiated Saxton Plutonium Fuel," WCAP-3385-56 Part II (July 1970).

15. J. Herczeg et al., BNL-NUREG-25607, Brookhaven National Laboratory, 1979.

16. M. L. Williams (ORNL), Memo to O. Ozer (EPRI),"EPRI-CELL Calculations with LASL ENDF/B-IV Cross Section," June 19, 1979.

SCHOOL OF NUCLEAR ENGINEERING

Atlanta, Georgia 30332 (404) 894-3720

E-26-645

September 14, 1979

MEMORANDUM

TO: C. R. Weisbin and M. L. Williams (ORNL)

FROM: J. M. Kallfelz and P. Levin

SUBJECT: Progress Report on Work for ORNL Subcontract 3986, Period August 1-September 10, 1979

1. Summary

1.1 Accomplishments for Report Period

- EPRI-CELL calculations for six mixed-oxide criticals [1,2] have been performed and analyzed. These calculations were repeated after the successful incorporation at ORNL of MacFarlane's disadvantage correction [3] and an improved thermal iteration scheme in EPRI-CELL. Our calculations thus yielded information on the influence of these improvements.

- CPM [5,6] has been initialized on the ORNL IBM-360, and cases for BAPL-1 [7] and three mixed oxide criticals [1,2] have been run at ORNL and/or on the Berkeley CDC-7600. The results are essentially identical for the two computers, and they have been analyzed and compared to results from EPRI-CELL, and those reported in NP-691 [2]. We have initiated a study of the problems of interfacing between NJOY [10] output and CPM input, which must be resolved to utilize ENDF/B-V cross sections in CPM.

1.2 Plans for the Work through September 30

- EPRI-CELL calculations for BAPL-1 through -3 [4,7] and the MO_2 lattices will be repeated with the modified version of the code, and analyzed. Investigations of isotopics of PWRs [11-13] utilizing EPRI-CELL will also be initiated.

- Work on the development of an interface between NJOY [10] and CPM will be continued.

2. EPRI-CELL Calculations

2.1 Results for Mixed Oxide Lattices

Table 1. presents EPRI-CELL results for ENDF/B-IV cross-sections [9] for six mixed-oxide lattices [1,2]. The six cases involve three different lattice pitches, with unborated and borated moderator for each pitch. Besides k_{eff}, the parameters reported are:

ρ_{28} = epi-thermal to thermal U-238 capture rate.

δ_{25} = epi-thermal to thermal U-235 fission rate.

δ_{28} = U-238 fission rate to U-235 fission rate.

CR = U-238 capture rate to U-235 fission rate.

The B^2 values used for the calculations are those of Table I of NP-691 [2]. The spatial mesh used for all the EPRI-CELL calculations had three, two, and three points in the fuel, clad, and moderator regions, respectively. This is the same number of points used by MacFarlane [14] in his analysis of BAPL-1. As we indicated in last month's report [4], BAPL-3 was repeated with a spatial mesh four times finer, giving negligible changes in its calculated parameters. Nonetheless, the mixed-oxide assembly pin radius and lattice pitches are somewhat larger than for BAPL-3, so this effect will be checked.

Unless indicated otherwise, all EPRI-CELL results reported in this memorandum are for an improved version of the code which made operational at ORNL on 31 August, which included an improved iteration scheme in the thermal range, and an option to calculate MacFarlane's disadvantage correction [3].

The results reported in NP-691 are also calculated using ENDF/B-IV cross sections. Experimental results for the above ratios are not reported

Table 1. Results for MO_2 Lattices from NP-691 and 196, for ENDF/B-4 Cross Sections

Lattice	k_{eff}		ρ_{28}		δ_{25}		δ_{28}		CR	
	EC[a]	NP[b]	EC	NP	EC	NP	EC	NP	EC	NP
U-L266 (low pitch)	.998	.983	5.41	5.11	.304	.288	.461	.441	3.40	3.28
U-L250 (low pitch, borated)	.990	.993	5.78	5.51	.326	.308	.482	.460	3.55	3.45
U-L189 (med. pitch)	.995	1.001	2.38	2.23	.127	.120	.257	.242	2.03	1.95
U-L212 (med. pitch, borated)	1.012	1.003	2.87	2.71	.154	.148	.295	.281	2.29	2.20
U-L282 (high pitch)	1.016	1.006	1.65	1.54	.0870	.0825	.196	.185	1.65	1.58[c]
U-L232 (high pitch, borated)	1.014	1.000	1.99	1.86	.106	.101	.228	.216	1.83	1.76[c]

(a) EPRI-CELL results, for Pu-239 $\chi(E)$, B1, with MacFarlane's disadvantage factor.

(b) Calculated results from NP-691. ANISN was used for the k_{eff} calculations, and presumably also for the other parameters.

(c) NP-691 values assumed to have only decimal point error, and hence multiplied by ten in this table.

for the mixed-oxide lattices. The document [2] indicates definitely that the k_{eff} results are from ANISN. We have been unable to determine positively that ANISN is also the code used for their other calculated results, although from the wording in the report [2] it appears probable that this is the case.

As can be seen, the k_{eff} values for EPRI-CELL (EC) and NP-691 (NP) differ up to about 1.5% for some cases. In general the NP results are closer to 1.0, particularly for the high pitch lattices. Possibly for these cases a refined mesh spacing will improve the EC results. The values for the reaction rate ratios are consistently higher for EC than for NP. For δ_{25}, δ_{28} and CR this could be caused by a lower U-235 fission rate for EC.

Calculations and analysis of these lattices will be continued to investigate the above effects.

2.2 Influence of Different Cross Sections and Methods for EPRI-Cell Calculations

Table 2. compares EPRI-CELL results for U-L266, using the NAI [8] and ENDF/B-4 [9] cross section libraries. The details of the generation of the NAI library are not clear to us, but we believe that MacFarlane's disadvantage correction (DISAD) should be applied; the table indicates NAI results with and without this correction. As can be seen, with the exception of δ_{25} the NAI reaction rate ratios are appreciably lower than those of ENDF/B-4, and the NP results of Table 1. Including DISAD reduces these ratios, while k_{eff} is increased by about 0.9%. A calculation of assembly U-L189 made by 26 August, when the DISAD routine was still being debugged, indicated a change in k_{eff} of 1.6% when this correction was applied.

Table 2. EPRI-CELL Results for MO_2 Critical #U-L266

	ENDF/B-4 DISAD[a]	NAI	
		DISAD	NO DISAD
k_∞	1.2800	1.3247	1.3137
k_{eff}	.9979	1.0318	1.0231
ρ_{28}	5.412	4.595	4.825
δ_{25}	.3044	.2969	.3061
δ_{28}	.4613	.4360	.4390
CR	3.401	3.037	3.139

(a) DISAD signifies that MacFarlane's disadvantage factor calculation has been included.

In comparing the results of Table 2 the difference in the basic data source of the two libraries should be considered. While we can not find a definite statement in the documentation, it appears thast most of this library is based on ENDF/B-II. However, there are exceptions, e.g. for our NAI calculations the U-238 cross sections were based on ENDF/B-I.

The following changes were observed in the results, for runs made before the 31 August version of the code was completed, but for which DISAD was not calculated. Using $\chi(E)$ from Pu-239 instead of U-235 decreased k_{eff} by 0.6% and 0.2%, for U-L189 and U-L266, respectively, and increased δ_{28} by about 7% for both these assemblies. Using the P1 option instead of B1 decreased k_{eff} by 1.2% for U-L189.

Finally, we compare in Table 3 the number of iterations to convergence in the thermal range for runs made with the "old" and "new" (31 August) version/iteration schemes. The "old" runs were made on 27 August, and did not include DISAD, while for the new runs DISAD was calculated. Since the print-out for the two convergence routines is not the same, we cannot compare the calculated convergence criteria.

3. CPM Calculations

3.1 BAPL-1 Results

This critical was calculated with CPM as a Pin-Cell (since it is an hexagonal lattice, and CPM treats square lattices only). The results are given in Table 4 along with previous EPRI-CELL* results (NAI cross-section library). There seems to be good agreement between calculations of k_∞ and k_{eff} (within 0.5%). The rest of the CPM results are for a critical spectrum, while the EPRI-CELL results are for the spectrum of the calculated k_{eff} (quite close to critical). The maximal deviation is less than

*Results obtained prior to the installment of MacFarlane's disadvantage factor in EPRI-CELL.

Table 3. No. of Iterations to Convergence[a]

Assembly	Old[a]	New[a]
U-L266	27	6
U-L250	38	6
U-L189	65	10
U-L212	77	10

a) See text

Table 4. Results of CPM BAPL-1 Pin-Cell Run Compared with EPRI-CELL Results[a]

A. Integral Parameters

	EPRI-CELL	CPM	
k_∞	1.1354	1.1356	(+.01%)[e]
k_{eff}	.99975	.99480	(-.5%)
		(Critical Spectrum)	
Absorptions[b]	.88053	.88305	(+.9%)
Leakage[b]	.11947	.11695	(-2.1%)
δ_{25}	.081[c]	.085[d]	(+4.3%)
ρ_{28}	1.353[c]	1.368[d]	(+1.13%)

B. Spectral Comparison

ϕ_g/ϕ_5 [f]	EPRI-CELL	CPM	
g = 1	.9425	.9390	(-.4%)
2	1.2838	1.2991	(+1.2%)
3	.9812	.9493	(-3.2%)[f]
4	.1208	.1380	(+14.2%)[f]
3 + 4	1.1020	1.0874	(-1.3%)

a) NAI Cross Section Library

b) Normalized to 1 neutron lost

c) 5 group EDIT
d) 2 group EDIT
(.625 eV cutoff)

e) Numbers in parentheses are the relative deviation of CPM from EPRI-CELL

f) The boundary between groups 3 and 4 is 1.855 eV and 2.10 eV for EPRI-CELL and CPM, respectively.

5%. There are some minor spectral changes, as indicated in Section B of the table.

The CPM fundamental mode was calculated in the B1 approximation. A rerun with the P1 approximation indicated very minor changes: k_{eff} is reduced by 0.5%. That is due mainly to a larger fast leakage (0.9% increase).

3.2 Mixed Oxide Criticals

The three unborated mixed oxide criticals (Nos. U-L266, -L189, -L282) [1,2] were calculated with CPM as pin cells. The geometrical details are similar to those used in EPRI-CELL (including the same number of points per region).

The results are given in Tables 5,6, and 7 compared with EPRI-CELL runs and NP-691 [2] results.

k_∞ of CPM is higher by 0.8-1.2% than the reference, (NP) [2], and is also higher by 0.9-2.3% than EPRI-CELL. For both comparisons the deviations decrease when the moderator to fuel ratio is increased. k_{eff} is less consistent, with deviations up to 2.4% from NP. The deviation from EPRI-CELL decreases from + 0.8% to - 0.3% with increasing pitch.

The results for the reaction rates deviate up to 8.5% from NP. The deviation from EPRI-CELL is smaller except for ρ_{28} (up to - 10.3%).

The thermal cell disadvantage factor $\bar{\phi}_M/\bar{\phi}_F$ as calculated in CPM is in agreement with THERMOS and HAMMER calculations (Table IXa of [2] as shown below:

	U-L266	U-L189	U-L282
Thermos	1.342	1.406	1.453
CPM	1.349	1.420	1.475
Hammer	1.373	1.430	1.483

Table 5. Comparison of CPM and EPRI-CELL* for MO_2 Critical #U-L266 (Pitch = 1.778 cm)

	CPM	EPRI-CELL	NP-691**
k_∞	1.3092	1.2800	1.2935
k_{eff}	1.0059	.9979	.9827
ρ_{28}	4.856	5.412	5.110
δ_{25}	.3042	.3044	.2876
δ_{28}	.4690	.4613	.4413
CR	3.173	3.401	3.278

Table 6. Comparison of CPM and EPRI-CELL* for MO_2 Critical #U-L189 (Pitch = 2.210 cm)

	CPM	EPRI-CELL	NP-691**
k_∞	1.3954	1.3761	1.3836
k_{eff}	.9940	.9949	1.0012
ρ_{28}	2.141	2.379	2.227
δ_{25}	.1270	.1268	.1201
δ_{28}	.2608	.2570	.2426
CR	1.927	2.034	1.952

*ENDF/B-4 Library, with MacFarlane's Disadvantage Factor

**Calculation using ENDF/B-4 data, presumably with ANISN

Table 7. Comparison of CPM and EPRI-CELL for MO_2 Critical #U-L282 (Pitch = 2.515 cm)

	CPM	EPRI-CELL*	NP-691**
k_∞	1.3778	1.3657	1.3666
k_{eff}	1.0135	1.0165	1.0059
ρ_{28}	1.497	1.654	1.543
δ_{25}	.0876	.0870	.0825
δ_{28}	.2007	.1962	.1850
CR	1.578	1.647	1.582***

*ENDF/B-4 Library, with MacFarlane's Disadvantage Factor

**Calculation using ENDF/B-4 data, presumably with ANISN

***Reported, apparently erroneously, as .1582 in NP-691

References

1. R.I. Smith and G.J. Konzek, "Clean Critical Experiment Benchmarks for Plutonium Recycle in LWRs, " EPRI NP-196, Electric Power Research Institute, April 1976.

2. R. Sher and S. Fiarman, "Analysis of Some Uranium Oxide and Mixed-Oxide Lattice Measurements," EPRI NP-691, Electric Power Research Institute, February 1978.

3. M. Segev, "Review of Cross Section Preparation Methods in EPRI-CELL," Memorandum to J.M. Kallfelz, C.R. Weisbin, and M.L. Williams, July 20, 1979.

4. J.M. Kallfelz, P. Levin and M. Segev, "Progress Report on Work for ORNL Subcontract 3986, Period July 1-31, 1979." Memo to C.R. Weisbin and M.L. Williams dated August 1, 1979.

5. "Advanced Recycle Methodology Program System Documentation," EPRI Report, CCM-3, Electric Power Research Institute, September 1977.

6. "The Collision Probability Module EPRI-CPM," Chapter 6 of Ref. 5.

7. H. Alter et al., "Cross Section Evaluation Working Group Benchmark Specifications," BNL-19302 (ENDF-202), Brookhaven National Laboratory, Revised September, 1978. Pages T(18-20)-1-3.

8. See Chapter 2, part II, of Ref. 5. The NAI generated EPRI-CELL libraries existing at ORNL were used: GAM library (FT03)-Tape #X14156;THERMOS library (FT04) - Tape #X03618

9. ENDF/B-IV - Based transport corrected EPRI-CELL libraries existing at ORNL were used: GAM library (FT03) - Tape #X05013;THERMOS library (FT04) - Tape #X20252.

10. R.E. MacFarlane et. al., "The NJOY Nuclear Data Processing System: User's Manual," LASL Report LA-7584-M (ENDF-272) 1978.

11. R.J. Nodvik et. al., "Supplementary Report on Evaluation of Mass Spectrometric and Radiochemical Analyses of Yankee Core I Spent Fuel, Including Isotopes of the Elements Thorium Through Curium," WCAP-6086 (September 1969).

12. J.B. Melehan, "Yankee Core Evaluation Program, Final Report," WCAP-3017-6094 (January 1971).

13. R.J. Nodvik, "Saxton Core II Fuel Performance Evaluation Part II, Evaluation of Mass Spectrometric and Radiochemical Analysis of Irradiated Saxton Plutonium Fuel," WCAP-3385-56 Part II (July 1970).

14. R.E. MacFarlane (LASL), memo to O. Ozer (EPRI) "Thermal Transport and Removal Cross Sections in EPRI-CELL," AOril 18, 1979.